

The Colocation Friction: Dual-Earner Job Search, Migration, and Labor Market Outcomes

Hanno Foerster* Robert Ulbricht†

November 22, 2025

Abstract

We develop a spatial directed search model to study job search and migration among dual-earner households. Using the model, we decompose observed gender gaps into exogenous gender differences, which are amplified by a “colocation friction” that is unique to dual-earner households. Estimated for the U.S. labor market, the colocation friction reduces women’s long-term migration gains by 19% and discourages mobility, particularly among “power couples”. The rise of remote work mitigates this friction, cutting average earnings losses by up to 50%.

Keywords: Dual-earner job search, gender inequality, migration, remote work, search frictions.

JEL Classification: E24, J16, J61, J64.

*Boston College, hanno.foerster@bc.edu

†Boston College, ulbricht@bc.edu

1 Introduction

A substantial share of U.S. workers belong to dual-earner households.¹ Compared to single-earner households, dual-earner households face a distinct constraint on their job search and labor mobility: the need to secure two jobs within the same location. Although underexplored in the literature, this constraint is likely to shape the labor market experience of dual-earner households (Mincer 1978).

In this paper, we develop a spatial search framework to formalize, characterize, and quantify how search frictions affect job search, migration, and labor market outcomes of dual-earner households. Building on Menzio & Shi (2010, 2011), search is directed, allowing household members to coordinate their search efforts toward the same locations. Yet, due to matching frictions, not every application generates a match and, due to the absence of employer coordination, matching succeeds independently across spouses. The lack of employer coordination, which we refer to as *colocation friction*, distinguishes job search of dual-earner households from the one by single earners.

We apply our framework to three main questions. First, we provide an exact decomposition of gender wage and employment gaps into exogenous gender differences in labor products, search efficiency, and job separation rates. Second, we quantify the contribution of the colocation friction to these gender gaps and its impact on domestic migration. Third, we examine how the rise of remote work reshapes labor market outcomes for dual-earner households and assess the extent to which it mitigates the colocation friction.

Quantification We calibrate our framework to the U.S. labor market. Households are characterized by each spouse's employment status, occupation, human capital, and the presence of children. Commuting zones vary in amenities, cost of living, childcare costs, and gender- and occupation-specific productivity levels. We calibrate these differences, combining household data from the American Community Survey (ACS) and the Current Population Survey (CPS) with geolocation data, commuting zone data from the Opportunity Atlas, and web-scraped data to inform the geography of the U.S. labor market. We estimate the model to further match occupation-level job and migration flows, the steepness of job-ladders, as well as the cross-sectional distribution of households over commuting zones.

Results The estimated model reproduces observed gender gaps in wages and employment without explicitly targeting them during the estimation. Specifically, men are 27% more likely to be employed and earn wages that are 31% higher than those of women. In our framework,

¹We define dual-earner households as married or cohabiting couples with both spouses in the labor force. In the 2010–2019 American Community Survey, they represent 66% of all such couples.

these gaps are fully attributable to four gender-specific factors: differences in productivity levels, productivity dispersion, job separation rates, and search efficiency. We provide an exact decomposition of gender gaps across these factors, finding that differences in productivity levels account for the largest share, followed by job separation rates.

Exogenous gender differences are amplified by the colocation friction in two ways. First, by preventing employer coordination, the friction increases the likelihood that migration creates trailing spouses, with possibly long-lasting career consequences. This effect is particularly pronounced among women, who — given calibrated productivity gaps — assume the trailing role in four out of five migrating households. As a result, gender gaps widen substantially after migration. Second, a higher prevalence of trailing spouses reduces the attractiveness of migration, lowering labor mobility and shaping households' long-run location choices.

To identify which households are most affected, we show that the colocation friction constrains job search if and only if a household's continuation value is convex in joint employment status changes. Intuitively, this is more likely for households with two employed spouses, when job ladders are steep, when migration costs are large, and when the search elasticity across locations is small. Conversely, the colocation friction is less likely to bind for non-employed households and those with children, particularly when childcare costs are high.

Quantitatively, the colocation friction reduces women's long-term migration gains by 19%, lowers migration rates by 13–17%, and accounts for 18% of the gender gap in migration earnings gains. Its impact is most pronounced among “power couples” with two employed spouses and above-average human capital, who exhibit highly convex continuation values. Overall, the colocation friction reduces average earnings by 2.7% for women and 0.9% for men.

Finally, we examine how the rise of remote work reshapes labor market outcomes for dual-earner households. Remote work relaxes the constraint that both spouses must secure employment in the same location, thereby mitigating the colocation friction. We simulate its introduction by allowing jobs to convert to remote positions at occupation-specific rates calibrated to match the observed remote job distribution. Following its introduction, migration initially declines sharply as households wait for remote conversion, then gradually recovers as more jobs become remote. Meanwhile, employment and earnings trend upward, especially for women, reflecting the easing of the colocation friction. In the long run, remote work can halve the earnings losses caused by the colocation friction, raising earnings by up to 1.4% for women and 0.4% for men.

Related literature The contribution of this paper is fourfold. First, we develop a novel spatial search model to study dual-earner households' job search and migration behavior. Our

model builds on directed search models by Menzio & Shi (2010, 2011), Menzio et al. (2016), Schaal (2017), and Herkenhoff et al. (2023), which we extend to incorporate dual-earner search and a spatial dimension. Modeling dual-earner search as directed rather than random is crucial, as it accounts for spouses' ability to coordinate their job search toward the same locations. Moreover, we benefit computationally from block recursivity (Menzio & Shi 2010; Wright et al. 2021), which makes our quantitative model tractable despite a large state and action space.

Second, we contribute to the literature on labor misallocation. Prior work has examined misallocation arising from search frictions (Hosios 1990), monopsony power (Galenianos et al. 2011; Rabinovich & Wolthoff 2022), spatial frictions (Sahin et al. 2014; Findeisen et al. 2021), and information frictions (Jovanovic 1979, 1984; Baley et al. 2022). Our paper introduces a novel source of misallocation: the colocation friction faced by dual-earner households.

Third, we add to a small literature analyzing dual-earner households' labor market and migration decisions, dating back to Mincer (1978).² This literature has explored how migration varies with household composition and gender-specific labor market opportunities (Costa & Kahn 2000; Lundberg & Pollak 2003; Guler et al. 2012; Lessem 2017; Braun et al. 2021; Alonzo et al. 2023; Gemici 2023; Glaeser et al. 2025; Rueda & Wilemme 2025), labor market policy (Venator 2025), and the geographic distribution of occupations (Román 2025). Relative to this work, our paper is the first to model dual-earner job search as directed, highlighting the colocation friction as the fundamental constraint. We are also first to estimate our framework at the commuting-zone level, in contrast to existing models calibrated at much coarser geographic levels.³

Finally, we contribute to the emerging literature on remote work and its labor market implications (Bagga et al. 2025; Berresheim 2025), by quantifying how remote work mitigates the colocation friction and reshapes migration and earnings dynamics for dual-earner households.

Roadmap The paper proceeds as follows. Section 2 introduces the model. Section 3 formalizes the colocation friction. Section 4 calibrates the model. Section 5 decomposes gender gaps. Section 6 computes the role of the colocation friction. Section 7 simulates the impact of remote work. Section 8 concludes.

²This literature is at the intersection of a somewhat larger literature studying dual-earner job search (e.g., Dey & Flinn 2008; Pilossoph & Wee 2021; Flabbi & Mabli 2018) and the literature on domestic migration, which typically focuses on single-earners (e.g., Kennan & Walker 2011; Kaplan & Schulhofer-Wohl 2017; Piyapromdee 2020).

³Existing dual-earner models with migration are typically calibrated to 2 or 9 locations. A notable exception is the model in Venator (2025), which is calibrated to the 48 mainland U.S. states.

2 General Framework

We develop a spatial search model of the labor market for dual-earner households. Search is directed, allowing household members to coordinate their search effort toward the same locations. Yet, due to frictional matching, spouses may fail to secure joint job offers in the same location within a given time frame. As a result, even under directed search, migration generates trailing spouses who experience unemployment following household relocation.

2.1 Environment

Preferences and technology Time is continuous and extends forever. There is a finite set of locations, indexed by $r \in \mathcal{R}$. The economy is populated by an endogenous measure of one-vacancy firms and a unit measure of households. Each household consists of two adult workers (or “spouses”), indexed by $i \in \{1, 2\}$, and zero or more children. While we will equate i with workers’ “gender” in our quantification, there is no need for now to make assumptions about the gender-composition within households. Firms and households are risk neutral and share the same effective discount rate ρ .

Following the literature, we assume that search and matching is privately efficient. In order to characterize labor and migration flows, it then suffices to specify the sum of a household’s instantaneous utility flow and the labor product of its employed members. Let

$$u(\mathbf{e}, \mathbf{s}, r) = \bar{u}(\mathbf{e}, \mathbf{s}, r) + \sum_{i \in \{1, 2\}} z_i(\mathbf{s}, r) \cdot \mathbb{1}_{e_i=1} \quad (1)$$

denote this joint value flow. Here, $\mathbf{e} \equiv (e_1, e_2) \in \{0, 1\}^2$ is the employment status of the household’s adult members, \bar{u} is their utility flow net of earnings, z_i is the labor product of spouse i , $r \in \mathcal{R}$ is the household’s current location, and $\mathbf{s} \in \mathcal{S}_1 \times \cdots \times \mathcal{S}_{n_s}$ is a generic “catch-all” state that captures other transitory and persistent characteristics of the household. For example, in our quantification, \mathbf{s} includes the occupation of both spouses, their human capital, and whether or not they have children. We assume that \mathbf{s} has finite support \mathcal{S}_k in all its dimensions $k \in \{1, \dots, n_s\}$.

Other than through search and migration, a household’s type $(\mathbf{e}, \mathbf{s}, r)$ evolves stochastically with Poisson arrival rates given by $\pi(\mathbf{e}', \mathbf{s}', r' | \mathbf{e}, \mathbf{s}, r)$. In our quantification, we specify π to expose households to exogenous job separations, human capital dynamics, location preference shocks, and the arrival and departure of children.

Labor markets and migration The labor market is organized in a continuum of submarkets indexed by the location of jobs $q \in \mathcal{R}$, the worker type (i, \mathbf{s}) , and the firm’s share y of

the joint value of the match.⁴ Workers direct their search toward these submarkets, choosing both a firm share y and a search effort $\kappa_{i,q}$ for each location q . Specifically, each spouse $i \in \{1, 2\}$ is endowed with a type-specific search budget $\bar{\kappa}_i(\mathbf{e}, \mathbf{s})$, which they can allocate to search across submarkets in different locations subject to

$$\left(\sum_{q \in \mathcal{R}} \kappa_{i,q}^{\frac{1+\eta}{\eta}} \right)^{\frac{\eta}{1+\eta}} \leq \bar{\kappa}_i(\mathbf{e}, \mathbf{s}). \quad (2)$$

Here, $\eta \geq 0$ is the elasticity of substitution between locations. In the limit where $\eta \rightarrow \infty$, workers allocate their entire search budget to the single location with the highest gains from search, as is usually the case in directed search models. At the other extreme where $\eta = 0$, diversifying search is costless and workers allocate $\bar{\kappa}_i(\mathbf{e}, \mathbf{s})$ units of search effort to each location with positive search gains as in the literature on multiple job applications (Albrecht et al. 2006; Kircher 2009; Galenianos & Kircher 2009).

Vacancies are created by an infinite supply of potential firms, which can open vacancies in any submarket at flow costs c . Vacancies and workers in a given submarket come together through a frictional matching process. In particular, a worker that allocates search effort $\kappa_{i,q}$ to submarket $\psi \equiv (q, y, i, \mathbf{s})$ meets a vacancy at rate $\kappa_{i,q}\lambda(\theta_\psi)$, where θ_ψ is the ratio between vacancies posted and the measure of workers' combined efforts in submarket ψ . Similarly, a vacancy posted in submarket ψ meets a worker at rate $\lambda(\theta_\psi)/\theta_\psi$. As usual, we assume that the contact function λ is twice differentiable, strictly increasing and concave, with $\lambda(0) = \lambda'(\infty) = 0$ and $\lambda'(0) = \infty$.

When a worker meets a firm, the firm offers a wage contract with present discounted value equal to the match value net of the firm's share y and hires the worker. Following Menzio & Shi (2010, 2011), we assume that the underlying contract space is complete. In particular, endogenous separations and on-the-job search maximize the joint value of the household and all its current employers.

Hires entail migration whenever the new job is in a location q that differs from a household's current location r . In this case, the spouse without the job offer quits their job and the household moves to q . Migration entails a utility cost $\chi(q|\mathbf{s}, r)$, normalized so that $\chi(r|\cdot, r) = 0$.

Discussion Three remarks are in order. First, while our analysis centers on dual-earner households, the model naturally generates labor force exits — non-employed individuals who exert zero search effort. In our calibration, women in households with children have the

⁴Indexing submarkets by firms' share y is equivalent to indexing by workers' lifetime utility along with households' employment status \mathbf{e} . While indexing by y allows us to eliminate \mathbf{e} from the submarket partition, the elimination is without loss as long as vacancies are created at constant returns to scale.

highest non-participation rate, at 18%, while exits among men are rare.⁵

Second, our model assumes that households reside in a single location. This assumption is motivated by the low prevalence of long-distance relationships in the United States.⁶ A potential concern is that such relationships might become more common around migration events. To examine this, we use data from the Panel Study of Income Dynamics and find no evidence that the frequency of long-distance relationships increases either before or after migration (see Appendix Figure A.I).

Third, one might ask whether households can secure job offers for both spouses simultaneously. One possibility is that prospective employers coordinate offers, as we explore in Section 3. Another is that offers can be stored over short horizons, effectively increasing the likelihood that both spouses hold offers at the same time. Our baseline model rules out these possibilities. In Section 4.3, we validate this restriction using indirect inference about dual-earner shares following migration events. Complementing evidence from DellaVigna et al. (2021) and Cortés et al. (2023), our indirect inference suggests that offer storage and offer coordination are negligible.

2.2 Equilibrium Characterization

Vacancy creation By free entry, the value of creating a vacancy must be zero in every submarket. That is,

$$c\theta_\psi = \lambda(\theta_\psi) \max\{0, y\}, \quad (3)$$

which pins down the market tightness θ_ψ as a function of y .

Search, migration, and separation Next, consider the search, migration and separation policies of workers. Private efficiency implies that the policies maximize the joint value of a household and its current employers, given by

$$\begin{aligned} \rho V(\mathbf{e}, \mathbf{s}, r) &= u(\mathbf{e}, \mathbf{s}, r) + \sum_{\mathbf{e}', \mathbf{s}', r'} \pi(\mathbf{e}', \mathbf{s}', r' | \mathbf{e}, \mathbf{s}, r) (V(\mathbf{e}', \mathbf{s}', r') - V(\mathbf{e}, \mathbf{s}, r)) \\ &\quad + \max_{\{\kappa_{i,q}, y_{i,q}\}} \sum_{i,q} \kappa_{i,q} \lambda(\theta_{i,q}) (V(\mathbf{e}^{\text{new}, i}, \mathbf{s}, q) - y_{i,q} - \chi(q | \mathbf{s}, r) - V(\mathbf{e}, \mathbf{s}, r)) \\ &\quad + \lim_{\epsilon \rightarrow \infty} \epsilon \sum_i \max \left\{ 0, V(\mathbf{e}^{\text{sep}, i}, \mathbf{s}, q) - V(\mathbf{e}, \mathbf{s}, q) \right\}. \end{aligned} \quad (4)$$

⁵The non-participation rate among women is close to that of prime-age partnered women in our 2010-2019 ACS sample, which is 23%.

⁶The share of married couples living apart between 2010 and 2019 is 0.026 in the CPS.

The joint value is composed of four terms: (i) the instantaneous value flow u as defined in (1); (ii) the value change induced by exogenous shocks to the household type $(\mathbf{e}, \mathbf{s}, r)$; (iii) the value change induced by either spouse finding a new job, which is maximized subject to the $\theta-y$ frontier posed by (3); and (iv) the option for either spouse to quit their job. Here, $\mathbf{e}^{\text{new},i}$ is a household's employment status after spouse i accepts a new job, defined by $e_i^{\text{new},i} = 1$ and $e_{-i}^{\text{new},i} = e_{-i} \cdot \mathbb{1}_{q=r}$ where “ $-i$ ” denotes the spouse without a job offer. Similarly, $\mathbf{e}^{\text{sep},i}$ is the employment status after spouse i quits their job, defined by $e_i^{\text{sep},i} = 0$ and $e_{-i}^{\text{sep},i} = e_{-i}$.

It remains to characterize the optimal choice of $\{\kappa_{i,q}, y_{i,q}\}$ in households' job search. Consider first the value split between households and firms. From (3), the market tightness is increasing in firms' share y , creating a trade-off for workers to search in submarkets with higher job-finding rates versus searching in submarkets where they retain a larger share of the surplus. Maximizing the third term in (4) subject to (3), the optimal market tightness is given by

$$\theta_{i,q}(\mathbf{e}, \mathbf{s}, r) = \lambda'^{-1} \left(\frac{c}{V(\mathbf{e}^{\text{new},i}, \mathbf{s}, q) - \chi(q|\mathbf{s}, r) - V(\mathbf{e}, \mathbf{s}, r)} \right), \quad (5)$$

which in turn pins down the matching rate per unit of search effort, $\lambda(\theta_\psi)$.

Finally, consider the allocation of search effort across locations, $\{\kappa_{i,q}\}$. Let $\Lambda_{i,q}$ denote spouse i 's expected gain per unit of search effort allocated to location q ,

$$\Lambda_{i,q}(\mathbf{e}, \mathbf{s}, r) \equiv \lambda(\theta_{i,q}^*) \left(V(\mathbf{e}^{\text{new},i}, \mathbf{s}, q) - \chi(q|r) - V(\mathbf{e}, \mathbf{s}, r) \right) - \theta_{i,q}^* c,$$

with $\theta_{i,q}^* \equiv \theta_{i,q}(\mathbf{e}, \mathbf{s}, r)$ denoting the optimal market tightness in (5). Maximizing the joint value (4) subject to the search budget (2), then yields

$$\kappa_{i,q}(\mathbf{e}, \mathbf{s}, r) = \Lambda_{i,q}(\mathbf{e}, \mathbf{s}, r)^\eta \left(\sum_v \Lambda_{i,v}(\mathbf{e}, \mathbf{s}, r)^{1+\eta} \right)^{-\frac{\eta}{1+\eta}} \bar{\kappa}_i(\mathbf{e}, \mathbf{s}). \quad (6)$$

Together with (5) this pins down job-finding and migration rates,

$$f_{i,q}(\mathbf{e}, \mathbf{s}, r) \equiv \kappa_{i,q}(\mathbf{e}, \mathbf{s}, r) \cdot \lambda(\theta_{i,q}(\mathbf{e}, \mathbf{s}, r)), \quad (7)$$

completing the characterization of search policies.

Steady state equilibrium In this economy, all policy rules are functions of only the idiosyncratic household type $(\mathbf{e}, \mathbf{s}, r)$. An equilibrium is a collection of maps from $(\mathbf{e}, \mathbf{s}, r)$ to search and separation policies satisfying (4)–(6) along with a value split satisfying (3). Unless otherwise mentioned, we focus on the case where the cross-sectional distribution over $(\mathbf{e}, \mathbf{s}, r)$

is at steady state.⁷

3 The Colocation Friction

Dual-earner households seeking to relocate without unemployment require a double coincidence of job offers. In our baseline economy, offers arrive independently across spouses, reflecting the absence of employer coordination to resolve this coincidence. We refer to this lack of coordination as *colocation friction*. This friction may harm dual-earner households in two ways. First, by creating trailing spouses, it reduces employment and earnings after migration. Second, as a consequence, it may discourage migration altogether.

Sections 5 to 7 quantify how the colocation friction shapes labor market outcomes. For context, this section first characterizes analytically when the friction binds. To do so, we construct a counterfactual economy where the arrival of spouses' job offers is correlated whenever this improves household welfare. This eliminates the double-coincidence problem, capturing the idea of employers coordinating, while preserving all other aspects of the search technology. Comparing the benchmark to the baseline, we then infer the friction to bind in any state where correlated matching is optimal.

3.1 Correlated Matching Benchmark

The correlated matching benchmark replicates the baseline economy but allows spouses to receive joint job offers at a destination-specific rate ω_q . Formally, consider two spouses that exert search efforts $\{\kappa_{i,q}\}_{i=1,2}$ to find jobs in submarkets $\{\psi_{i,q}\}_{i=1,2}$ in some location q . Given ω_q , the spouses obtain a joint job offer in $\psi_{1,q}$ and $\psi_{2,q}$ at rate ω_q , and obtain individual offers at the residual rates $\kappa_{i,q}\lambda(\theta_{\psi_{i,q}}) - \omega_q$.

The benchmark is characterized by a joint assignment of correlation rates, search efforts, and submarkets to households,

$$\mathcal{C} : (\mathbf{e}, \mathbf{s}, r, V) \mapsto \{\omega_q\}_{q \in \mathcal{R}}, \{\kappa_{i,q}, \psi_{i,q}\}_{i,q \in \{1,2\} \times \mathcal{R}}.$$

Crucially, households are indexed by a continuation value function V in addition to their current state, enabling us to apply the benchmark to the steady state of the baseline economy as well as any transition path. The benchmark assignment \mathcal{C} maximizes households' lifetime

⁷The cross-sectional distribution is characterized by a standard Kolmogorov forward equation, detailed in Appendix A.2.

utility subject to the feasibility constraint

$$0 \leq \omega_q \leq \min_{i \in \{1,2\}} \left\{ \kappa_{i,q} \lambda(\theta_{\psi_{i,q}}) \right\} \quad \text{for all } q \in \mathcal{R}. \quad (8)$$

We note that the benchmark does not change the primitives of the search technology. That is, workers face the same constraint (2) on their allocation of search effort $\{\kappa_{i,q}\}$, firms face the same cost of vacancy creation c , and matching is subject to the same frictional matching function λ . As a result, both economies share the same feasibility frontier for *total matches*, differing only in how those matches can be distributed across households.

3.2 When Is the Colocation Friction Binding?

We say that for a household of type $(\mathbf{e}, \mathbf{s}, r)$ with continuation value V , the colocation friction binds for job searches in location q if and only if matching would optimally be correlated in the counterfactual economy, $\omega_q(\mathbf{e}, \mathbf{s}, r, V) > 0$. The following proposition characterizes when this is the case.

Proposition 1. *Fix a continuation value function V . Let*

$$\Delta V_{i,q}(\mathbf{e}, \mathbf{s}, r) = V(\mathbf{e}^{\text{new}, i}, \mathbf{s}, q) - \chi(q | \mathbf{s}, r) - V(\mathbf{e}, \mathbf{s}, r)$$

denote the gains from an individual match by spouse i . Similarly, let

$$\Delta V_q^{\text{corr}}(\mathbf{e}, \mathbf{s}, r) = V(\mathbf{e}^{\text{corr}}, \mathbf{s}, q) - \chi(q | \mathbf{s}, r) - V(\mathbf{e}, \mathbf{s}, r)$$

denote the gains from a correlated match, where $\mathbf{e}^{\text{corr}} = (1, 1)$. Then correlated matching is beneficial if and only if

$$\Delta V_q^{\text{corr}}(\mathbf{e}, \mathbf{s}, r) > \sum_{i \in \{1,2\}} \Delta V_{i,q}(\mathbf{e}, \mathbf{s}, r). \quad (9)$$

If condition (9) holds, the correlated matching rate is optimally set to its upper bound, $\omega_q = \min_{i \in \{1,2\}} \left\{ \kappa_{i,q} \lambda(\theta_{\psi_{i,q}}) \right\}$. Otherwise, it is optimally set to its lower bound, $\omega_q = 0$.

The formal proof is in Appendix A.1. Intuitively, as illustrated in Figure 1, condition (9) evaluates the curvature of $V - \chi$ with respect to the number of job offers in a given location q . If this mapping is convex, the household benefits from increasing risk by coordinating job offers, making the colocation friction binding. Conversely, if the mapping is concave, the household is better off hedging by keeping job offers statistically independent, rendering the colocation friction slack.

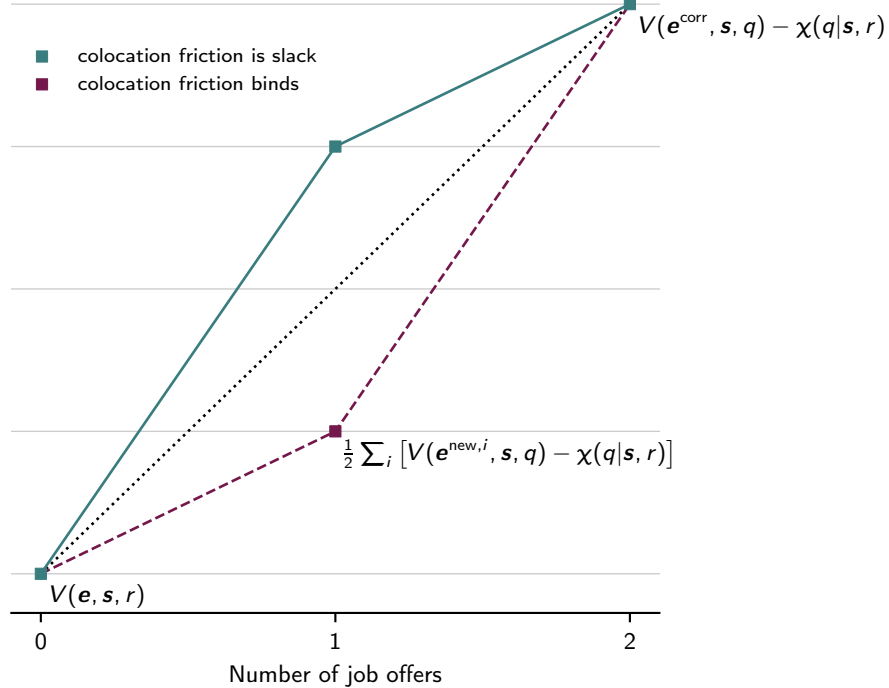


Figure 1: Illustration of condition (9). The colocation friction binds if and only if, averaged across spouses, $V - \chi$ is convex in the number of simultaneous job offers as in the dashed graph, and is slack if $V - \chi$ is concave as in the solid graph.

3.3 Simple Example

Before quantifying our framework, we briefly explore a simple example to illustrate the economic forces that determine the curvature of V . Consider a household with initial type $(\mathbf{e}_0, \mathbf{s}_0, r_0)$. There are no exogenous shocks, $\pi(\cdot|\cdot) = 0$, and both spouses and all locations $q \neq r_0$ are symmetric. Specifically, we have $\bar{\kappa}_i(\mathbf{e}, \mathbf{s}) = \bar{\kappa}$, $\chi(q|\mathbf{s}, r) = \chi$, and

$$u(\mathbf{e}, \mathbf{s}, r) = \begin{cases} u_0 & r = r_0 \\ u_{e_1+e_2} & r \neq r_0, \end{cases}$$

with $u_0 + \rho\chi \leq u_1 \leq u_2$. Finally, we simplify by considering the limit where the matching function is inelastic in vacancies, $\lambda(\theta) = \lim_{\gamma \rightarrow 0} \theta^\gamma$.

The example admits a simple recursive solution where $V(\mathbf{e}, \mathbf{s}, r) \in \{V_0, V_1, V_2\}$. Specifically, if $r \neq r_0$ and both spouses are employed, we have $\rho V_2 = u_2$. If $r \neq r_0$ and only one spouse is employed, we have $\rho V_1 = u_1 + \bar{\kappa}(V_2 - V_1)$. Finally, the initial value at $r = r_0$ is given by

$$\rho V_0 = u_0 + 2\bar{\kappa}N^{\frac{1}{1+\eta}}(V_1 - \chi - V_0),$$

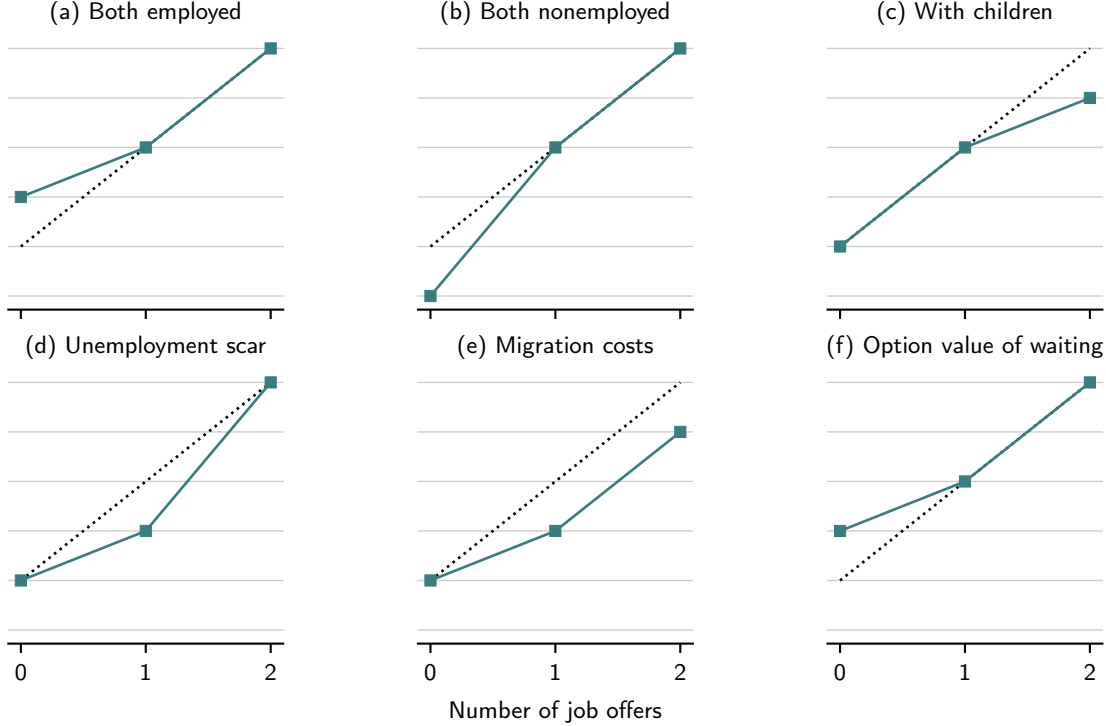


Figure 2: Illustration of economic forces shaping the curvature of $V - \chi$. The colocation friction is slack in the cases depicted in panels (b) and (d), and binds in the other cases.

where N is the number of locations $q \neq r_0$.

Economic forces behind the colocation friction Evaluating condition (9) for the simple example, the colocation friction binds if and only if

$$\frac{u_0 + \Omega(N^{\frac{1}{1+\eta}})}{2} + \frac{u_2 - \rho\chi}{2} \geq u_1 - \rho\chi \quad (10)$$

with

$$\Omega(x) = 2\bar{\kappa} \left(\frac{x-1}{\rho + 2\bar{\kappa}x} \right) \left(u_1 - u_0 - \rho\chi + \frac{\bar{\kappa}}{\rho + \bar{\kappa}} (u_2 - u_1) \right).$$

The condition reveals several distinct factors affecting the curvature of $V - \chi$, illustrated in Figure 2. First, consider the case where there are no migration costs, $\chi = 0$, and search effort is infinitely elastic across locations, $\eta \rightarrow \infty$. In this case, condition (10) simplifies to $(u_0 + u_2)/2 \geq u_1$, so the curvature of $V - \chi$ in the number of simultaneous job offers is entirely determined by the curvature of u .

In particular, given u_1 and u_2 , V is more convex for larger u_0 , reflecting that the colocation friction is more likely to bind for households with a high initial value flow such as when both spouses are employed (illustrated in Panel a of Figure 2). Conversely, the colocation friction is

more likely to be slack for households with a low initial value flow such as when both spouses are non-employed (Panel b).

Similarly, given u_0 and u_2 , V is more convex the smaller u_1 (Panel d). Intuitively, this captures, in reduced form, economies where falling off the job ladder comes with high costs; e.g., due to human capital depreciation (e.g., Jung & Kuhn 2019), deteriorated bargaining positions (e.g., Cahuc et al. 2006; Lise & Robin 2017), or slippery bottom job rungs (Jarosch 2023). All of these mechanisms increase the cost of becoming a trailing spouse, making it more likely that the colocation friction binds. Conversely, factors reducing the value flow of dual employment u_2 , such as having children when childcare costs are large, reduce the convexity of V and make it less likely that the colocation friction binds (Panel c).

Next, consider the case where migration costs are strictly positive, $\chi > 0$. As illustrated in Panel (e), this trivially introduces convexity in the search gains, making it more likely that the colocation friction binds. Intuitively, this is because migration costs accrue regardless of whether the household has one or two job offers at hand, which raises the relative returns of having two job offers.

Finally, consider the case where the search elasticity across locations η is finite (Panel f). In this case, there is an option value of delaying migration reflected in $\Omega(N^{\frac{1}{1+\eta}}) > 0$. Intuitively, with $\eta < \infty$, there are efficiency gains from broadening search to multiple locations. After migrating, these efficiency gains are lost when the trailing spouse narrows their search to the location of the leading spouse.⁸ Again, this introduces convexity and makes it more likely that the colocation friction binds.

4 Quantitative Model

We now introduce the quantitative model and calibrate it to the U.S. labor market. The quantitative model is a special case of the general framework in Section 2, with locations corresponding to U.S. commuting zones and households being differentiated by several characteristics beyond their employment status and residence.

4.1 Setup

Household heterogeneity We quantify our model for dual-earner households whose adult members are composed of one woman, indexed by $i = f$, and one man, indexed by $i = m$. Households are differentiated by a vector $s = (o_f, o_m, h_f, h_m, k)$, which along with households' employment status and their location defines their type (e, s, r) . Specifically, each spouse i

⁸This is true regardless of whether repeated migration occurs along the equilibrium path. In either case, because search and migration costs are sunk, there is a positive option value of delaying migration if η is finite.

is characterized by an immutable occupation, o_i , and a time-varying human capital level, $h_i \in \{\underline{h}, \bar{h}\}$. In addition, we differentiate households with and without children, $k \in \{0, 1\}$.

Shocks Beyond search and migration, household types $(\mathbf{e}, \mathbf{s}, r)$ evolve stochastically through several independent shocks. The arrival rates of shocks are indexed by households' *occupation vector*, $\mathbf{o} \equiv (o_f, o_m)$, allowing them to vary across households.

First, jobs are destroyed at an exogenous, gender-specific rate $\delta_i(\mathbf{o})$. Second, children enter and exit households at rates $\pi_{k\uparrow}(\mathbf{o})$ and $\pi_{k\downarrow}(\mathbf{o})$, respectively. Third, human capital appreciates or depreciates as a function of a worker's current employment status: Employed workers' human capital appreciates to $h_i = \bar{h}$ at rate $\pi_{h\uparrow}(\mathbf{o})$, while non-employed workers' human capital depreciates to $h_i = \underline{h}$ at rate $\pi_{h\downarrow}(\mathbf{o})$. Finally, households are exposed to location preference shocks (detailed below) that induce them to relocate from commuting zone r to q at rate $\pi_{q|r}(\mathbf{o})$.

Preferences and technology The instantaneous utility and labor product are given by

$$u(\mathbf{e}, \mathbf{s}, r) = \sum_{i \in \{f, m\}} \underbrace{\left\{ h_i z_i(o_i, r) \cdot \mathbb{1}_{e_i=1} + b_i z_i(o_i, r) \cdot \mathbb{1}_{e_i=0} \right\}}_{\text{labor product + home production}} + \underbrace{a(k, r) - p(r)}_{\text{amenities - rent}} - \underbrace{\xi(r) \cdot \mathbb{1}_{k=e_f=e_m=1}}_{\text{childcare cost}}$$

Here, $z_i(o_i, r)$ is a gender-, occupation- and commuting-zone-specific productivity that scales the labor and home products, $h_i z_i(o_i, r)$ and $b_i z_i(o_i, r)$. The value of living in commuting zone r is further determined by the value of its amenities $a(k, r)$, which differs by child status k , its cost of living $p(r)$, and its childcare costs $\xi(r)$. The latter accrue only if a household has children and both spouses are employed.

4.2 Calibration

We calibrate the model using household data from the American Community Survey (ACS) and the Current Population Survey (CPS), which we combine with geolocation data, commuting zone data from the Opportunity Atlas (Chetty et al. 2025) and our own web-scraped data that inform the geography of the U.S. labor market. Appendix B.1 describes the data sources in detail.

Geography We consider all commuting zones (CZ) in the 48 contiguous states, excluding a few isolated commuting zones for which we lack the data to construct our amenity measure.

For computational efficiency, we merge commuting zones that are close geographically and in terms of all observational characteristics. We describe the details of our merging algorithm in Appendix B.4. Starting from 720 commuting zones with non-missing data, we obtain a final data set of 546 commuting zones post-merge.

Location preference shocks We design the arrival rates of location preference shocks, $\pi_{q|r}(\mathbf{o})$, to match the cross-sectional distribution of occupation vectors \mathbf{o} over commuting zones. To do so in a computationally feasible way, we assume that location shocks induce a lump-sum utility shift,

$$\tau(\mathbf{e}, \mathbf{s}, r, q) = -\left(V(\mathbf{e}, \mathbf{s}, q) - \chi(q|\mathbf{s}, r) - V(\mathbf{e}, \mathbf{s}, r)\right),$$

that makes a household exactly indifferent to migrate from q to r .⁹ With this design, households' value function and search policies, characterized by (4), are independent of the distribution of location shocks $\{\pi_{q|r}(\mathbf{o})\}$. For a given model parameterization, we can thus solve for V and the endogenous search and migration policies in a first step, and then design $\pi_{q|r}(\mathbf{o})$ in a second step to match, at the steady state, the empirical distribution over commuting zones.

We do so by choosing the distribution of shocks $\{\pi_{q|r}(\mathbf{o})\}$ with the smallest total prevalence that still allows us to exactly match the empirical distribution over commuting zones and occupation vectors. Our algorithm does so in a computationally efficient way: On an Intel i7-9700 computer, solving for V , identifying the set $\{\pi_{q|r}(\mathbf{o})\}$ that matches the empirical distribution over \mathbf{o} , and solving for the implied ergodic distribution over $(\mathbf{e}, \mathbf{s}, r)$ takes about 2.5 seconds.

Assigned parameters We parameterize the model at a monthly frequency. Households retire and are replaced by new households at a monthly rate of 0.021/12, chosen so that the average household's work life lasts for 47 years. The effective discount rate ρ is set to the retirement rate plus 0.05/12, corresponding to an annual time preference rate of 5%.

We categorize households using the occupation classification by Autor & Dorn (2013).¹⁰ To economize on states, we drop occupations that are pursued by less than 3% of workers

⁹To avoid indirect effects on the employment distribution, we assume that location shocks do not alter the employment status \mathbf{e} .

¹⁰Specifically, we differentiate occupations by the six top-level occupation classifications in Autor & Dorn (2013): (1) managers/professionals/technicians/finance/public safety, (2) clerical/retail sales, (3) low-skill services, (4) production/craft, (5) machine operators/assemblers, (6) transportation/construction/mechanics/mining/farm. Henceforth, we reference these occupation categories using shortened labels.

Table 1: Frequency distribution over occupation vectors

o_f/o_m	Managers/prof/tech	Clerical/retail sales	Low-skill services	Production/craft	Machine operators	Construction/farm	Total
Managers/prof/tech	.32	.06	.03	.02	.02	.10	.55
Clerical/retail sales	.11	.04	.02	.01	.01	.09	.28
Low-skill services	.04	.02	.03	.01	.01	.06	.17
Total	.47	.12	.08	.04	.04	.25	1.00

Notes.—Frequencies are among dual-earner households in the ACS. Rows correspond to women’s occupation and columns to men’s occupation, classified following Autor & Dorn (2013).

Table 2: Average wage by occupation and gender

Occupation	Women	Men
Managers/prof/tech	1.57	2.45
Clerical/retail sales	.81	1.25
Low-skill services	.52	.70
Production/crafts	—	1.35
Machine operators	—	1.05
Construction/farm	—	1.12

Notes.—Wages are normalized relative to the median ACS wage. Occupations are classified following Autor & Dorn (2013).

per gender.¹¹ This yields 18 occupation vectors, $(o_f, o_m) \in \{1, \dots, 3\} \times \{1, \dots, 6\}$, that cover 93.5% of all dual-earner households in the ACS. Tables 1 and 2 show their frequency distribution and average wages.

We set the job separation rates $\delta_i(\mathbf{o})$ to the empirical employment to non-employment rates in the CPS, measured at the gender \times occupation-level. We use a Cobb-Douglas matching function, $\lambda(\theta) = \theta^\gamma$, with matching elasticity $\gamma = 0.2$, as estimated by Lange & Papageorgiou (2020). We set the search elasticity across locations to $\eta = 0$, so search effort is inelastic across submarkets, as in Albrecht et al. (2006), Kircher (2009) and Galenianos & Kircher (2009). For computational efficiency, we limit workers to a maximum of four simultaneous searches and verify ex post that the restriction is locally non-binding almost everywhere.¹²

Next, we normalize the high human capital realization to $\bar{h} = 1$ and set $b_m = 0.4$, so the ratio between home and labor product equals 0.4 for high- h men (c.f., Shimer 2005). We then

¹¹Following this criterion, we drop three out of six top-level occupations for women (“production/ craft”, “machine operators”, and “construction/ farm”) and do not drop any occupations for men.

¹²We verify this in the calibrated model by increasing the maximum number of simultaneous searches to five. We find that less than 0.001% of workers search in more than four markets simultaneously.

set $b_f = b_m \cdot E[z_m]/E[z_f] = 0.625$, so the average home product is the same across genders. With b pinned down, we set $\underline{h} = b_m = 0.4$, capturing the idea that low- h men are marginally attached to the labor market. Whether low- h men join the labor force then depends on the value gain from future human capital appreciation versus the childcare costs that incur if they have children and their spouse is employed.

Our calibration of local productivities, $z_i(o_i, r)$, exploits that for almost all (i, o_i, r) the median worker in our model has high human capital.¹³ With this in mind, we infer the local productivities $z_i(o_i, r)$ from the gender \times occupation-specific median wages in a commuting zone r , as measured in the ACS.¹⁴ We set their scale to normalize economy-wide average earnings to 1.

Next, we use average rents for two bedroom apartments to inform the cost of living $p(r)$ for each commuting zone. We set childcare costs $\xi(r)$ to 8.5% of the median household income in each commuting zone, consistent with the average, age-weighted household expenditures on childcare documented by Guner et al. (2020). We set the monthly arrival rate of children to the fertility rate among childless households in the ACS, $\pi_{k\uparrow} = 0.075/12$. We then use the departure rate of children to match the share of households with children in the ACS, which is 56%, yielding $\pi_{k\downarrow} = (0.56^{-1} - 1) \cdot \pi_{k\uparrow}$ net of the retirement rate.¹⁵

Finally, we combine several existing and web-scraped data sources to inform the local amenity values $a(k, r)$. Our data include information on crime rates, various climate and weather categories, walkability scores, measures of beach access and quality, and various data on infrastructure, such as hospital quality and school quality measures. We assume that all school-related measures are valued by households with children, while all other amenities are valued by all households. Appendix B.3 describes the data in detail.

One challenge in calibrating the amenity value is that $a(k, r)$ enters $u(\mathbf{e}, \mathbf{s}, r)$ in *income-equivalent* units, requiring us to convert the various data into income-equivalent units. To do so, we assume that regional differences in income-equivalent amenities have the same

¹³Intuitively, the median worker is determined by the appreciation and depreciation rates $\pi_{h\uparrow}$ and $\pi_{h\downarrow}$, which we estimate below to match the *average* unemployment scar in the data. Given $\bar{h} - \underline{h}$, which is about five times the size of the average impact scar, our estimated process implies that the majority of workers has “high” (or, more accurately, “median”) human capital. We verify numerically that conditional on (i, o_i, r) , the median workers are indeed of type \bar{h} for almost all gender \times occupation \times commuting zone combinations.

¹⁴Equating productivities with wages is model-consistent for two separate reasons. First, for labor contracts to be self-enforcing in the absence of contractual commitments on the worker-side, workers must be paid their labor product at all times other than during the instant they are hired (see, e.g., Menzio & Shi 2011; Baley et al. 2022). Second, while our calibration uniquely pins down the vacancy cost c relative to search budgets $\bar{\kappa}_i(\mathbf{e}, \mathbf{s})^{(1-\gamma)/\gamma}$, their absolute value is indeterminate. Without loss of generality, we can thus consider the limit where both $c \rightarrow 0$ and $\bar{\kappa}_i(\mathbf{e}, \mathbf{s}) \rightarrow 0$, in which case workers are always paid their labor product under the unique equilibrium labor contract.

¹⁵To be consistent with our “perpetual youth” setting, we re-weight the ACS sample when computing the fertility rate and the share of households with children so that age is distributed geometrically in the sample.

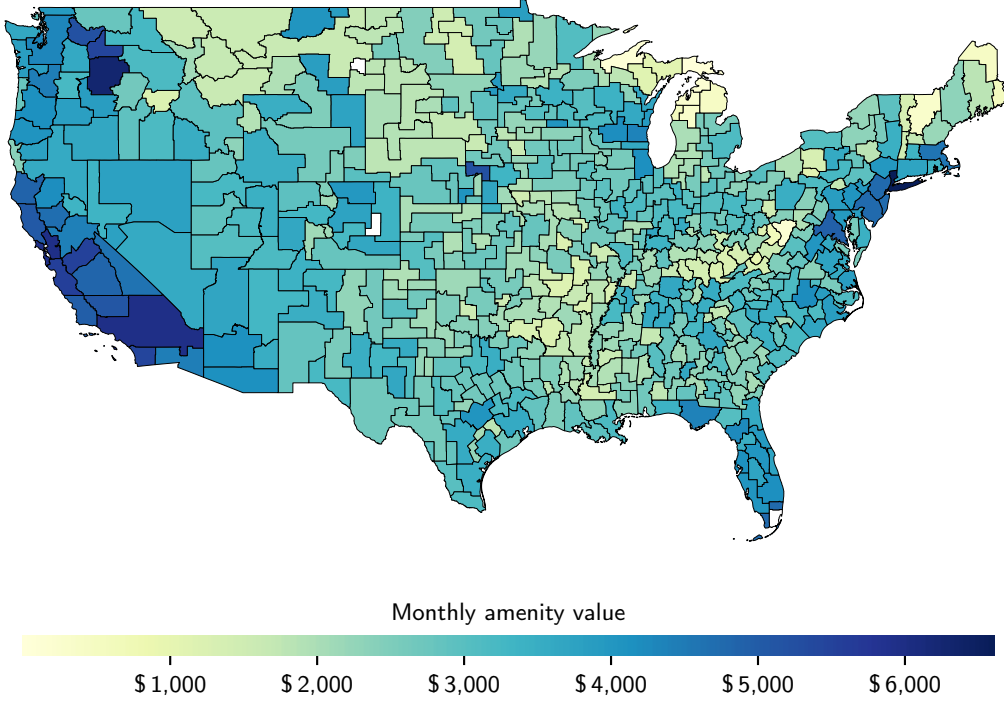


Figure 3: Income-equivalent amenity values for households without children. Amenity values are normalized to have a minimum of zero. White patches mark commuting zones with missing data.

passthrough rate on local rents as regional differences in wages, and that the passthrough of school quality scales with the local share of households with children. Given these assumptions, we can infer the amenity value from the following regression:

$$p_r = \beta_0 + \epsilon \cdot (\bar{w}_r + \beta'_1 \mathbf{a}_r^{\text{all}} + \beta'_2 \bar{k}_r \mathbf{a}_r^{\text{kids}}) + v_r, \quad (11)$$

where p_r are average rents in commuting zone r , \bar{w}_r is the local median household income, \bar{k}_r is the local share of households with children, and $\mathbf{a}_r^{\text{all}}$ and $\mathbf{a}_r^{\text{kids}}$ collect our various amenity data (applicable to all households and only for households with children, respectively). We estimate a passthrough rate ϵ of 0.161, which is consistent with there being significant mobility frictions (as our framework indeed delivers). Given our estimate for ϵ , we infer the local amenity values as

$$a(k, r) = a_0 + \beta'_1 \mathbf{a}_r^{\text{all}} + \beta'_2 \mathbf{a}_r^{\text{kids}} \cdot \mathbb{1}_{k=1},$$

for some constant a_0 . Without loss of generality, we normalize a_0 so that $\min_r a(0, r) = 0$.¹⁶ Figure 3 plots the estimated amenity values for $k = 0$.

We summarize all exogenously assigned parameters in Table 3.

¹⁶Constant shifts in $a(k, r)$ translate to constant shifts in V by a_0/ρ and are thus of no consequence.

Table 3: Assigned parameters

Parameter	Value	Source
Time preference rate, annualized	.05	literature
Retirement rate, annualized	.021	avg. working life of 47 years
Home production, b_m, b_f	.4, .625	Shimer (2005), ACS
High human capital, \bar{h}	1.0	normalization
Low human capital, \underline{h}	.4	same as b_m , see text
Search elasticity across locations, η	.0	literature
Matching elasticity, γ	.2	Lange & Papageorgiou (2020)
Child arrival rate $\pi_{k\uparrow}$, annualized	.075	ACS
Child departure rate $\pi_{k\downarrow}$, annualized	.038	ACS
Job separation rates, $\{\delta_i(\mathbf{o})\}$	see text	CPS
Local productivities, $\{z_i(o_i, r)\}$	see text	ACS
Cost of living, $\{p(r)\}$	see text	Atlas
Child care costs, $\xi(r)$	see text	Guner et al. (2020)
Amenities, $\{a(k, r)\}$	see text	Atlas, web scraped

Estimated parameters We calibrate the remaining parameters using the method of moments, with weights chosen to minimize the relative distance between model and empirical moments. All model moments are computed at the steady state. Our estimation leverages that the steady state distribution is generated by 18 non-communicating Markov chains, separated by occupation vectors \mathbf{o} . In choosing target moments and parameters that are also indexed by \mathbf{o} , we can therefore split the estimation into 18 subproblems, greatly reducing the computational complexity. As usual, conditional on \mathbf{o} , all parameters are identified jointly. In the following, we provide a heuristic mapping from moments to parameters to guide intuition.

In our model, the strength of search frictions is determined by the search budgets relative to the vacancy cost, $\bar{\kappa}_i(\mathbf{e}, \mathbf{s})/c^{\gamma/(1-\gamma)}$, which are not separately identified. For some arbitrary normalization of c , we parameterize $\bar{\kappa}_i(\mathbf{e}, \mathbf{s}) = g_\kappa(i, \mathbf{o})$, and use it to match the empirical job-finding rate out of unemployment in the CPS, measured at the gender \times occupation-pair level. To be consistent with the data, we only consider non-employed workers that are actively searching for jobs when computing the job-finding rate in the model.

Next, following Jung & Kuhn (2019) and Jarosch (2023), we estimate the human capital appreciation and depreciation rates, $\pi_{h\uparrow|e}(\mathbf{o})$ and $\pi_{h\downarrow|u}(\mathbf{o})$, to match the empirical steepness of job ladders. To do so, we simulate the wage scar of male workers separated from their job at $t = 0$ relative to the control group of non-separated workers, $\log(w_t^{\text{treat}}/w_t^{\text{control}})$, and match it to the estimated wage scars in Huckfeldt (2022) for $t = 12$ and $t = 36$ months.

It remains to calibrate the migration costs $\chi(q|\mathbf{s}, r)$. To do so, we differentiate between “work-related” migration, which in the model corresponds to the endogenous migration through job search, and other “residual” migration, captured in the model through location shocks. On the empirical side, we consider 45% of all observed migration as work-related, based on

Table 4: Summary of target moments

Moment	Level	No. of moments	Source	\approx maps to
Job-finding rate	$o_f \times o_m \times \text{gender}$	36	CPS	$\bar{\kappa}_i(\mathbf{o})$
Wage scar, 1 & 3 yrs	$o_f \times o_m \times \text{year}$	36	Huckfeldt (2022)	$\pi_{h\uparrow}(\mathbf{o}), \pi_{h\downarrow}(\mathbf{o})$
Migration rate, by bin	$o_f \times o_m \times \text{bin}$	144	ACS	$\chi(q \mathbf{o}, r)$
Distribution over CZs	$o_f \times o_m \times r$	9828	ACS	$\pi_{q r}(\mathbf{o})$

Notes.—Due to adding up constraints on target distributions, the number of linearly independent moments is reduced by 36, matching the number of estimated parameters.

the survey evidence in Maurer (2017).¹⁷

With this distinction, we calibrate migration costs by targeting, for each occupation vector \mathbf{o} , both the rate of work-related migration and its distribution in the ACS. Specifically, most migration in the data occurs at short distances and between commuting zones with similar population sizes. To capture these facts, we parameterize $\chi(q|\mathbf{s}, r)$ in terms of the spatial distance between any two commuting zones' population-weighted centroids, $d^{\text{geo}}(r, q)$, and the absolute difference in their population sizes, $d^{\text{pop}}(r, q)$. Specifically, we set

$$\chi(q|\mathbf{o}, r) = \sum_{k \in \{\text{geo, pop}\}} \sum_{j \in \{1, \dots, 4\}} \chi_j^k(\mathbf{o}) \cdot \mathbb{1}_{d^k(r, q) \in \text{Bin}_j^k},$$

with four geographic and four population bins, $\{\text{Bin}_j^{\text{geo}}, \text{Bin}_j^{\text{pop}}\}_{j=1}^4$, chosen to capture the cross-bin variation in migration rates (cf. Figure 5). For each occupation vector \mathbf{o} , we normalize $\chi_1^{\text{geo}}(\mathbf{o}) = 0$ and then estimate the seven remaining cost parameters, $\{\chi_j^k(\mathbf{o})\}$, to match the total work-related migration rate of occupation vector \mathbf{o} as well as its frequency distribution over the four geographic and the four population bins.

Table 4 summarizes the moments targeted in our estimation.

4.3 Model fit

Targeted moments Our algorithm ensures that the model exactly replicates the household-by-occupation vector distribution across commuting zones. Figures 4 and 5 compare the remaining 216 moments with their empirical targets. The model achieves a close fit for these moments as well.

Untargeted moments For independent validation, we compare the estimated model's predictions for employment rates and gender wage gaps with their empirical counterparts, both at the steady state and following migration events.

¹⁷This is closely in line with our own calculation based on a corresponding survey question in the CPS, which indicates that 47% of across-state migration is for a new job or a job transfer.

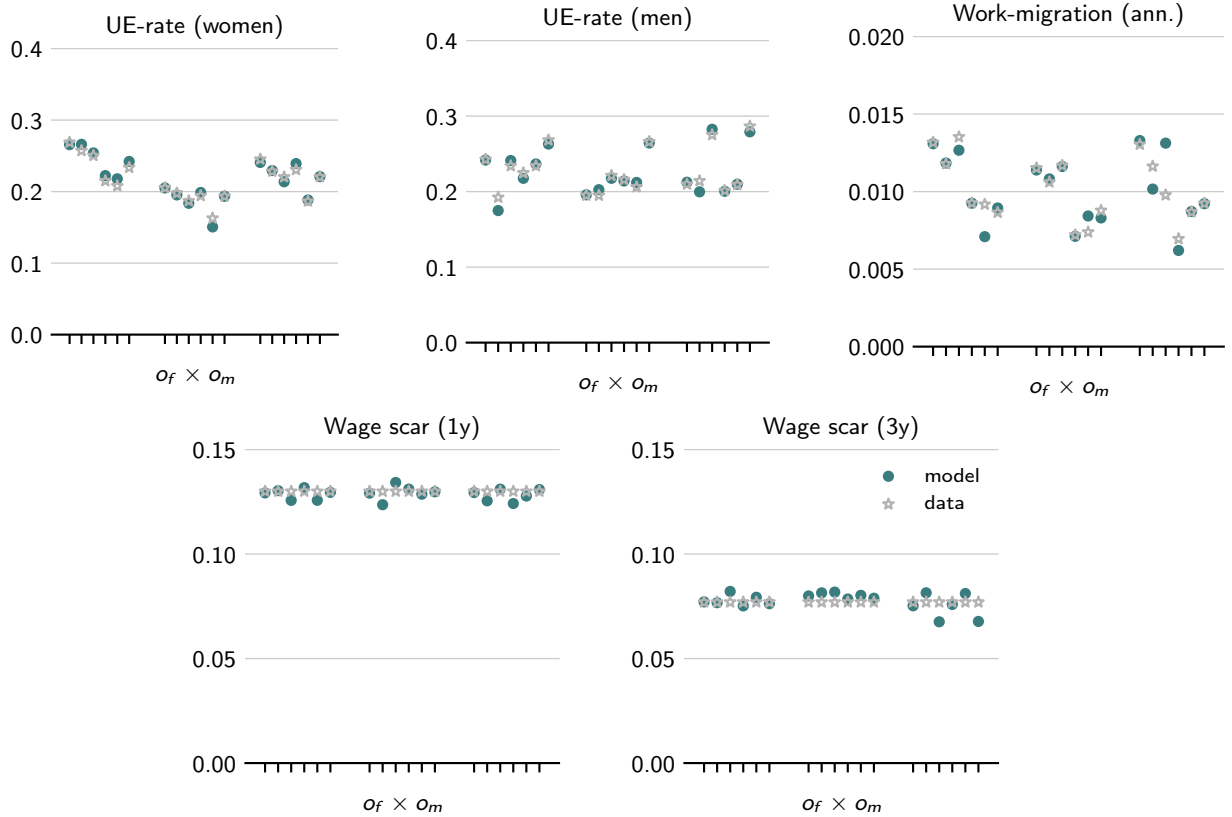


Figure 4: Targeted moments 1: Job-finding rates, annualized migration rates, and wage scars by occupation vectors. Occupation vectors are grouped by women’s occupation, $o_f \in \{1, 2, 3\}$, with individual ticks corresponding to men’s occupation, $o_m \in \{1, \dots, 6\}$.

First, consider the steady-state moments (Table 5, Columns 2 and 3). As expected, the estimated model nearly replicates the gender wage gap, which is closely linked to the calibrated productivities.¹⁸ More noteworthy is that the model also closely matches steady-state employment rates. These reflect labor force participation decisions shaped by the share of low- h workers, their relative home versus market productivity, the option value of gaining work experience, and childcare costs — all calibrated independently of employment rates.

Next, consider the same moments after migration. Because trailing spouses often find jobs within weeks of moving, comparing gender gaps at the instant of migration ($t = 0$) to time-aggregated data would be misleading. To address this, we compare the model with data three months post migration (Table 5, last two columns). Again, employment rates and gender gaps align closely with their empirical analogs.

¹⁸The wage gaps fall toward the upper end of those reported in the literature (see Doepke & Tertilt 2016 for an overview). This is because we include part-time workers in all wage calculations, both, when calibrating productivities and when computing the empirical gaps.

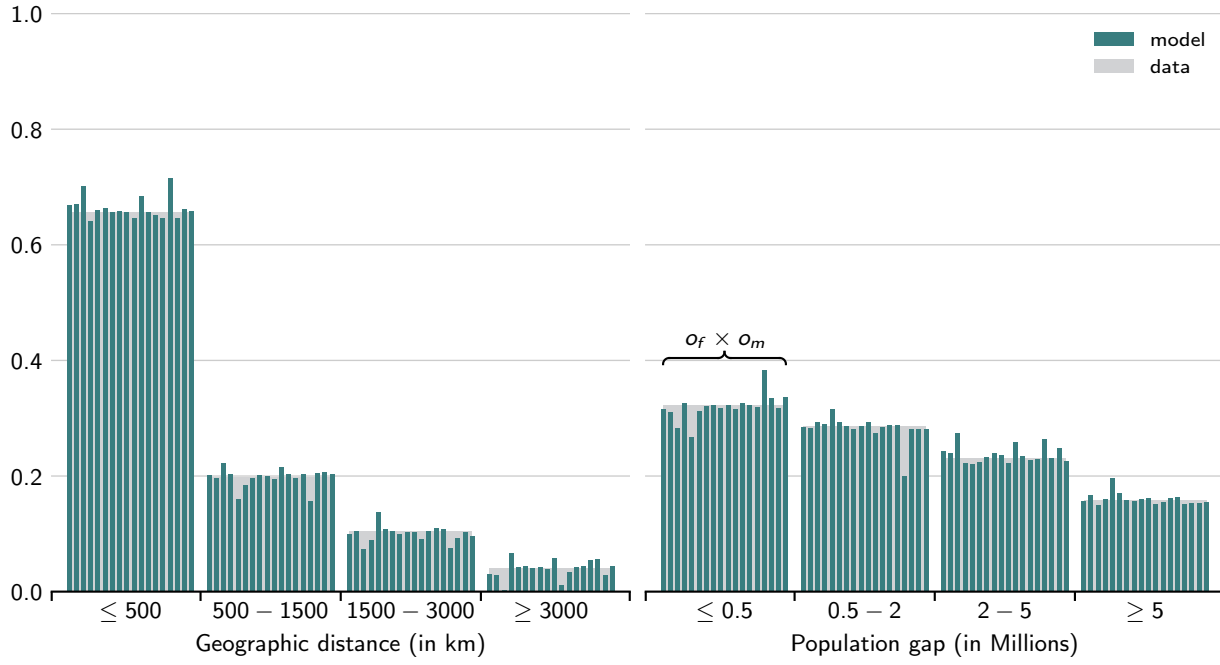


Figure 5: Targeted moments 2: Migration frequency over geographic distance and population gap.

Offer storage and coordinated matching This comparison indirectly tests our assumption that the baseline model excludes offer storage and coordinated matching. If these options were prevalent, the share of dual-employed households would be higher immediately after migration and remain elevated three months later. However, the estimated model almost perfectly replicates the observed dual-employed share at three months (Table 5, bottom row), suggesting little scope for offer storage or coordinated matching in our setting.

Table 5: Untargeted moments: Employment rates and gender gaps

Moment	Steady state		Post Migration ($t = 0$)		Post Migration ($t = 3$)	
	Model	Data	Model	Data	Model	Data
Earnings gap	.46	.45	.80	n/a	.60	.68
Wage gap	.31	.34	.30	n/a	.41	.49
Employment rate						
women	.73	.73	.22	n/a	.60	.59
men	.93	.88	.78	n/a	.87	.91
Dual-employed share	.68	.65	.00	n/a	.48	.52

Notes.—Gender gaps are defined as $1 - E[x_f]/E[x_m]$. Empirical moments are computed in the PSID, unconditionally and 3 months after a work-related migration event has been reported.

5 Dual-Earner Migration and Gender Inequality

As shown in Table 5 above, gender inequality is substantial and becomes even more pronounced after migration. Measured in earnings, the steady-state gap is 46%, which widens to 80% immediately following migration — largely because in four out of five migration events, women are the trailing spouse. As a result, the model implies that the three-year present value gain from migration is substantially larger for men than for women: 0.13 versus 0.02 (in units of average lifetime earnings).¹⁹ We now explore the causes of these gaps.

Decomposing gender inequality In our calibration, three inputs are gender-specific: productivities $z_i(\cdot)$, job separation rates $\delta_i(\cdot)$, and job-finding rates. The first two enter the model directly, while the third informs the estimation of search capacities $\kappa_i(\cdot)$. In the absence of gender differences in z_i, δ_i, κ_i , the model would not generate any gender gaps.

To assess the contribution of each input to the estimated gender gaps, we re-simulate the model, equalizing these parameters across genders in all possible permutations. We further break down the role of productivity differences by separately equalizing the average productivity level and the dispersion of productivities across commuting zones, giving us four gender-specific inputs in total. Our decomposition is exact and is independent of the order of variation.

Formally, denote a permutation of the four gender-specific inputs by

$$\mathbf{x} = (\mathbb{1}_k)_{k \in \{1, \dots, 4\}} \in \{(0, 0, 0, 0), (0, 0, 0, 1), \dots, (1, 1, 1, 1)\},$$

where $\mathbb{1}_k$ indicates that input k is equalized across genders by setting the corresponding parameter for women to the one for men. Given a permutation \mathbf{x} with $\mathbf{x}_k = 0$, the marginal contribution of input k to gap \mathcal{G} is given by

$$d_k \mathcal{G}(\mathbf{x}) = \mathcal{G}(\mathbf{x} + \mathbb{1}_k) - \mathcal{G}(\mathbf{x}).$$

Our decomposition averages the marginal contribution for each input across permutations. To ensure that the decomposition adds up exactly to the total contribution, we weigh each of these permutations by the number of paths connecting from $(0, 0, 0, 0)$ to $(1, 1, 1, 1)$ through $(\mathbf{x}) \rightarrow (\mathbf{x} + \mathbb{1}_k)$. That is,

$$contrib_k = \sum_{\mathbf{x} \in \{\mathbf{x}: \mathbf{x}_k = 0\}} w(\mathbf{x}) \cdot d_k \mathcal{G}(\mathbf{x})$$

¹⁹We compute these gains by simulating a representative sample of migrating households and comparing it with the same sample absent migration.

Table 6: Decomposition of gender gaps

	Steady state		Post Migration		
	Employment gap	Wage gap	Employment gap	Wage gap	Leading spouse gap
Productivities (level)	17 %	28 %	40 %	17 %	17 %
Productivities (dispersion across CZs)	1 %	1 %	9 %	8 %	3 %
Job-finding rates	-4 %	-1 %	9 %	4 %	2 %
Job-separation rates	8 %	3 %	15 %	1 %	5 %
Total	21 %	31 %	72 %	30 %	28 %

Notes.—Post-migration gaps are computed immediately after migration ($t = 0$). Employment and wage gaps are defined as $1 - E[x_f]/E[x_m]$. The leading spouse gap is defined as the share of work-related relocations in which the man is the leading spouse, in excess of 50%.

with

$$w(\mathbf{x}) = \frac{\overbrace{\left(\sum_l \mathbf{x}_l \right)!}^{\text{paths in}} \times \overbrace{\left(n - \sum_l \mathbf{x}_l - 1 \right)!}^{\text{paths out}}}{\underbrace{n!}_{\text{all paths}}}, \quad n = 4.$$

Table 6 summarizes the average marginal contributions, contrib_k . Level differences in productivity explain most of the gender gaps. Equalizing average productivities, men would lead 60% (instead of 78%) of moves. Larger job separation rates for women account for most of the remaining gap, while job-finding rates and productivity dispersion matter mainly for the post-migration gaps.

Is the main earner always the leading spouse? Given that wage levels explain most of the leading-spouse gap, it is natural to ask whether the main earner, defined as the spouse with the higher labor product, $h_i z_i(o_i, r)$, typically leads the move. Table 7 shows that this is true for main-earning men, but not for main-earning women, who trail their spouses in about half of all moves.

This pattern aligns with evidence from Jayachandran et al. (2024), who find that cross-CZ moves improve men’s labor market outcomes more than women’s, regardless of which spouse has the greater earnings potential. In our model, this arises because men face larger productivity differences across CZs and accumulate more human capital post-migration, amplifying their returns to relocating.

Heterogeneity by occupation Another natural question is whether leading-spouse gaps persist across occupations. Table 8 indicates that they largely do: Men lead most moves regardless of their own or their spouse’s occupation. Women lead a substantial share only

Table 7: Leading spouse by main earner status

	Man is leading spouse	Woman is leading spouse
Man is main earner	92.0 %	8.0 %
Woman is main earner	45.6 %	54.4 %

Notes.—Shares of migration events led by men and women, conditional on who is the main earner. Rows sum to 100%.

Table 8: Leading spouse by occupation vector

o_f/o_m	Managers/prof/tech	Clerical/retail sales	Low-skill services	Production/craft	Machine operators	Construction/farm
Managers/prof/tech	87 %	67 %	27 %	65 %	48 %	49 %
Clerical/retail sales	97 %	85 %	72 %	87 %	80 %	80 %
Low-skill services	98 %	90 %	81 %	94 %	87 %	83 %

Notes.—Share of migration events led by men. Rows correspond to women's occupation and columns to men's occupation, classified following Autor & Dorn (2013).

when they hold a high-paying occupation — such as in management, technology, or finance — while their spouse works in a low-paying occupation, such as low-skill services, construction or farming.

The role of children Finally, we examine how children affect migration. Table 9 shows that households with children migrate less often than childless households. In our framework, this reflects two forces: First, younger, childless households are less well matched and therefore have stronger incentives to relocate. Second, the arrival of children shifts amenity preferences and lowers the opportunity cost of having a trailing spouse, who can provide childcare.²⁰ The second force increases migration among households with children, but is dominated by the first force, implying an overall higher migration rate among childless households. This is consistent with evidence from the ACS, where childless households migrate at roughly twice the rate of households with children.

²⁰While we do not explicitly model age, households enter our model without children, so that average time in the model does indeed correlate with child status.

Table 9: Work-related migration with and without children

	Model	Data
Children	.35 %	1.05 %
No children	2.09 %	2.26 %

Notes.—Annualized migration rates by child status. Data are cross-CZ migration rates in the ACS, scaled by the CPS share of migration due to new jobs or job transfers.

Table 10: Consequences of migration for earnings

	ΔPV in 3-year earnings		ΔPV in lifetime earnings	
	Baseline economy	No colocation friction	Baseline economy	No colocation friction
Women	.021	.084	.296	.366
Men	.129	.148	.610	.632

Notes.— ΔPV denotes difference in the present value of earnings between a representative sample of migrating households and an identical sample without migration, denominated in units of economy-wide average lifetime earnings.

6 Quantifying the Colocation Friction

At the steady state distribution, the colocation friction binds in nearly all non-local searches ($q \neq r$) and is slack in most local searches ($q = r$). Having shown that gender inequality widens after migration, we now assess the extent to which the colocation friction drives this widening, beginning with its direct effect on migrating households.

6.1 Direct Effect on Migrating Households

To provide context, we first quantify returns to migration in the baseline economy. To do so, we simulate earnings gains for a representative sample of migrating households and compare them to an identical sample absent migration. Table 10 shows the difference in the present value of earnings between these two groups.

Over the first three years after migration, men's present value gain equals 0.129 (in units of average lifetime earnings), compared to only 0.021 for women. In the longer run, the gap narrows but remains substantial: 0.610 for men versus 0.296 for women. These gaps largely reflect the leading-spouse gap discussed earlier, amplified by slowing human capital accumulation for the trailing spouse.

To isolate the causal effect of the colocation friction, we next consider the same migrating sample of households, but now simulate hypothetical present value gains when the colocation friction is relaxed by allowing for joint job offers as implied by the correlated matching

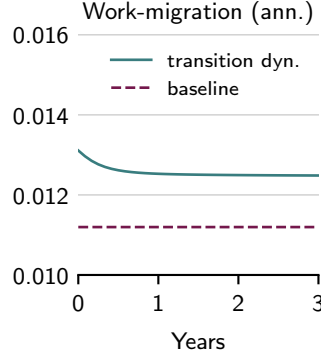


Figure 6: Impact of the colocation friction on work-related migration. The dashed line shows the annual steady-state migration rate in the estimated model. The solid line shows the rate for a representative sample of households for whom the friction is relaxed from $t = 0$ onward.

benchmark.²¹ As expected, relaxing the colocation friction barely changes men’s gains, but dramatically increases women’s short-term earnings.

Overall, the friction reduces women’s migration gains by 0.070 (again, in units of average lifetime earnings), with most losses (0.063) accruing in the first three years. In relative terms, this reduces women’s long-term migration gains by 19% and accounts for 18% of the corresponding gender gap.

6.2 Discouraged Migration

Beyond post-migration outcomes, the colocation friction also influences migration decisions, consistent with Mincer’s (1978) hypothesis.²² To quantify its impact on migration rates, we relax the colocation friction for a representative, measure-zero sample of households and their descendants, and study the resulting migration behavior. Figure 6 shows that relaxing the friction raises migration rates by 17% initially and by 13% in the long run, indicating a sizable effect on aggregate mobility.²³

To understand the determinants of this increase in mobility, we next examine which households are discouraged from migrating when the friction is active. To do so, Table 11

²¹Specifically, here we keep both the migrating sample of households and their migration destinations fixed, changing only the employment status immediately following migration according to the hypothetical correlation policies $\omega_k(e, s, r, V)$ implied by the correlated matching benchmark with V equal to its steady-state value in the baseline economy.

²²While similar in its implication, the underlying logic in Mincer (1978) is distinct, reflecting the fact that if spouses rank locations differently, then their average gain from migration is less than that of a single-earner.

²³Note that by relaxing the friction perpetually, momentary migration incentives are reduced by the option value of migrating without friction in the future. Alternatively, we can measure the “compound effect” of the colocation friction on momentary migration rates by relaxing the friction during only a short time window and then reimpose it after. In this case, migration increases by over 60% to an annual rate of 1.86% while the friction is relaxed.

Table 11: Comparison of baseline migrants to discouraged migrants

	Migrating	Discouraged	Population average
Children	.14	.31	.56
Both employed	.38	.92	.68
Both non-employed	.22	.00	.02
Household income	1.21	2.20	2.00
Employment rate			
women	.52	.96	.73
men	.64	.96	.93
Human capital			
women	.77	1.00	.75
men	.89	.99	.87
Local productivity			
women	.92	.99	1.00
men	1.31	1.32	1.54

Notes.—Displayed are averages for three household groups: (i) Migrating: households who migrate in the baseline economy. (ii) Discouraged: households who do not migrate in the baseline economy, but migrate when the colocation friction is relaxed. (iii) Population average: all households, weighted by the steady-state distribution.

contrasts households that migrate under the baseline with those that only migrate when the friction is removed. In line with the stylized model in Section 3.3, discouraged households tend to be dual-employed, high-income, and high-human-capital, resembling the stereotypical “power couple” (Costa & Kahn 2000). By contrast, baseline migrants are more likely to be childless and lower-income, making the friction less consequential for them.

Regarding the returns to migration, both groups have below-average local productivities, especially for men. Nevertheless, because human capital and productivity are complementary, discouraged households have significantly higher potential returns from migration. Consequently, earnings losses from discouraged migration are substantial: 0.140 for women and 0.168 for men (in units of average lifetime earnings). It is worth noting that while women bear most direct costs of the colocation friction, indirect effects from forgone migration opportunities affect both genders roughly equally.

6.3 Combined effect

To summarize, we quantify the overall impact of the colocation friction, taking into account the direct effect on post-migration employment, discouraged migration, as well as location choices. To do so, consider again the sample of households for whom we have relaxed the colocation friction at $t = 0$. Figure 7 plots transition dynamics in their earnings, employment, local productivity, and human capital. Relaxing the colocation friction immediately boosts women’s employment and earnings, with further gains accruing through human capital

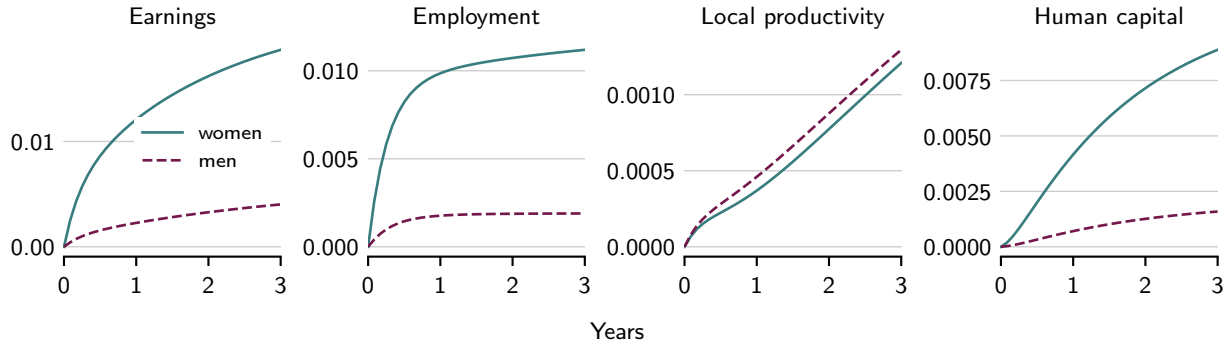


Figure 7: Impact of the colocation friction on earnings, employment, local productivities, and human capital. The plots show log-differences between a representative sample of households for whom the friction is relaxed from $t = 0$ onward and the steady state where the friction is active.

Table 12: Overall losses attributed to colocation friction

	Women	Men
Earnings	2.70 %	.86 %
Employment	1.29 %	.19 %
Local productivity	.54 %	.53 %
Human capital	1.18 %	.20 %

Notes.—Losses are computed by comparing average earnings in the baseline economy with the correlated matching benchmark. Both economies are evaluated at their respective steady-state distribution.

accumulation and relocation to higher-productivity regions. By contrast, the combined effect of the colocation friction on male earnings is more subdued.

Overall, the friction reduces women's steady-state earnings by 2.7% and men's by 0.9%, and further lowers amenity values equivalent to an additional 1% earnings loss. Table 12 further decomposes the earnings losses into employment (1.3% for women, 0.2% for men), productivity losses from forgone relocation (0.5% for both), and human capital losses (1.2% for women, 0.2% for men).

7 Remote Work

We now study how the emergence of remote work reshapes dual-earner households' job search and migration behavior. By enabling workers with remote jobs to relocate without losing employment, remote work has the potential to mitigate the colocation friction.

7.1 Model Extension

We incorporate remote work into the quantitative model described in Section 4.1. Apart from the modifications detailed below, the model remains unchanged.

Modeling remote work We model remote work as a job-level attribute that can evolve over the course of a match. Specifically, each job begins as non-remote and becomes remote at rate $\phi_i(\mathbf{o})$. Once a job becomes remote, it remains so for the duration of the match.

The defining feature of remote jobs is their portability across locations. If one spouse holds a remote job, they remain employed even if the household relocates to another commuting zone. Remote work thus relaxes the constraint that both partners must secure employment within the same location.

Mainly for tractability, we assume that the productivity of remote jobs is determined by the residence of workers.²⁴ This assumption also serves a modeling purpose: it isolates the role of remote work in mitigating the colocation friction without directly affecting wages, providing a clean counterfactual.

Calibration of job conversion rates The additional parameters that require calibration are the rates $\{\phi_i(\mathbf{o})\}$, at which non-remote jobs become remote. We calibrate these rates to match the occupation-level shares of jobs that can be performed entirely at home, as reported by Dingel & Neiman (2020). To align with our model’s occupation structure, we aggregate these shares to the coarser occupational classification in Autor & Dorn (2013). Table 13 presents the aggregated shares.

We map these shares into conversion rates $\{\phi_i(\mathbf{o})\}$ by assuming that the share of remote jobs in each occupation is in steady state. That is,

$$\text{remote share}(o_i) = \frac{\phi_i(\mathbf{o})}{\phi_i(\mathbf{o}) + \delta_i(\mathbf{o})}, \quad (12)$$

where δ_i is the calibrated job separation rate.²⁵ Inverting equation (12) yields $\phi_i(\mathbf{o})$.

7.2 Implications of Remote Work

We now simulate the introduction of remote jobs. We initialize the economy at the steady state of the baseline without remote work. From $t = 0$ onward, jobs begin converting to remote jobs at the calibrated conversion rates $\{\phi_i(\mathbf{o})\}$. In the following, we explore the impact on migration and earnings along the transition path and at the new steady state.

²⁴The assumption is tractable as it does not require tracking the origin location of jobs. Instead, we can track households’ remote status using only two indicators $\text{remote}_f, \text{remote}_m \in \{0, 1\}^2$. While the empirical determinants of remote workers’ productivity remain the subject of ongoing debate (Bloom et al. 2015; Gibbs et al. 2023; Emanuel & Harrington 2024; Barrero et al. 2023), evidence by Brinatti et al. (2021) suggests that remote wages indeed adjust with the residence of workers.

²⁵In principle, equation (12) would also need to account for endogenous separations. However, since remote jobs survive migration, endogenous separations are negligible compared to δ_i .

Table 13: Share of remote workable jobs by occupation

Occupation	% potentially remote
Managers/prof/tech	57 %
Clerical/retail sales	55 %
Low-skill services	15 %
Production/crafts	—
Machine operators	—
Construction/farm	2 %
Women	49 %
Men	35 %

Notes.—Shares are computed by aggregating the occupation-specific shares of remote-workable jobs reported by Dingel & Neiman (2020) to the occupation classification by Autor & Dorn (2013). No remote workable jobs are reported for production/crafts and machine operators. The bottom panel aggregates these remote shares using the occupation–gender distribution in Table 1.

Migration rates Remote work affects both the optimal timing and the long-run incidence of migration. Figure 8a plots migration rates along the transition path, following its introduction at $t = 0$. Migration initially drops by 28%, caused by the option value of waiting for a remote job before relocating. As the incidence of remote jobs rises, so does the migration rate. Specifically, among households with at least one remote job, migration initially surges by 38% relative to their counterparts in the baseline economy (Figure 8b).²⁶ Over time, as these households relocate to preferred commuting zones, their migration rate declines, closing the gap to their baseline counterparts.

Households without remote jobs exhibit the opposite trend (Figure 8c). Caused by the option value of waiting, their migration rates initially fall, leading to increased geographic mismatch. This mismatch raises the potential gains from migration, which increases migration rates (solid line) as well as the option value of waiting (gap between solid and dashed line). At the remote economy’s steady state, the option value reduces migration among non-remote households by 45%.

Taken together, aggregate migration converges to 7% below the baseline steady state, accounted for by the option value of waiting, partially offset by increased migration gains.

Composition of migrating households Table 14 further dissects the composition of migrating households in the remote economy’s steady state. For comparison, columns 2 and 3 replicate the corresponding statistics from the baseline economy (cf. Table 11). Migrants with at least one remote job are typically dual-employed, high-income, and high-human-capital households — closely resembling the power couples who, in the baseline economy, were

²⁶Formally, the comparison controls for selection in (e, s, r) conditional on at least one spouse having a remote job, by computing migration in the baseline economy given the same conditional distribution over (e, s, r) at each point in the transition path.

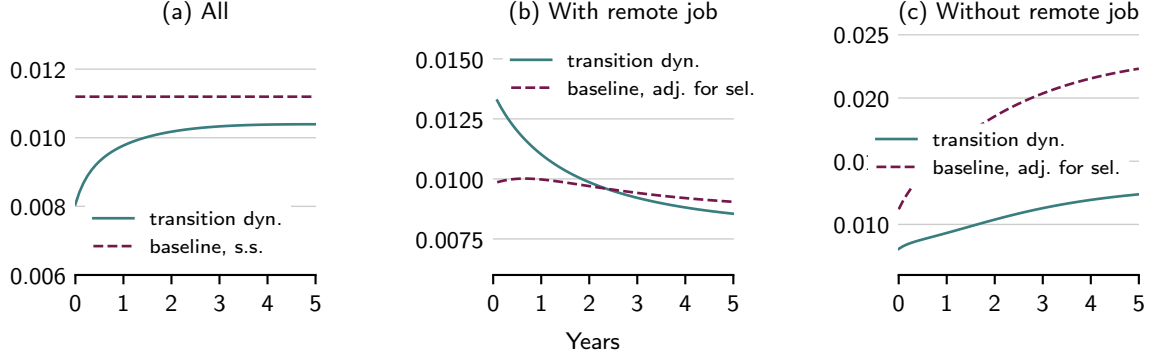


Figure 8: Transition dynamics following the arrival of remote work at $t = 0$. Panel (a) shows the annualized work-related migration rate along the transition path. Panels (b) and (c) break up the migration rate by remote status. Dashed lines correspond to migration in the baseline economy, computed at the steady state (panel a) and controlling for selection in (e, s, r) conditional on remote status and time t (panels b and c).

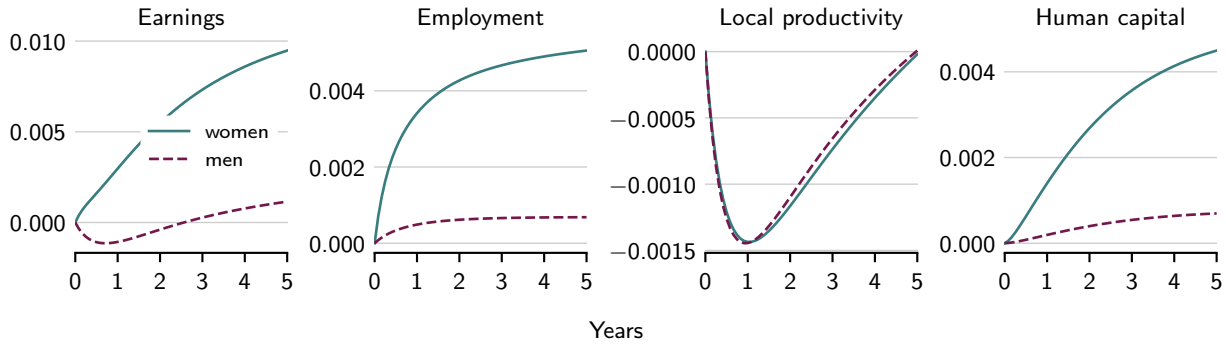


Figure 9: Impact of remote work on earnings, employment, local productivities, and human capital. The plot shows log-differences between a representative sample of households for whom positive transition rates to remote jobs are introduced from $t = 0$ onward and the steady state without remote work.

discouraged from migrating due to the colocation friction. In contrast, migrants without remote jobs exhibit average human capital and below-average employment levels, similar to the typical migrants in the baseline economy. Thus, the introduction of remote work shifts the migrant composition away from the baseline sample toward power couples with higher migration gains.

Earnings Figure 9 plots earnings and its components along the transition path. Overall, earnings trend up in the long run, driven by three factors. First, the ability to relocate without job loss for one's spouse directly increases employment and earnings, particularly for women, who are more likely to be trailing spouses. Second, the shift in migration toward power couples boosts earnings for both genders, due to complementarities between human capital and local productivity. Third, opposing these effects, postponed migration among non-remote households results in forgone earnings gains, explaining the initial decline in

Table 14: Composition of migrants: baseline vs. remote work scenario

	Baseline economy		Remote work economy		
	Migrating	Discouraged	All migrating	Migrating w/ remote job	Migrating w/o remote job
Children	.14	.31	.16	.26	.10
Both employed	.38	.92	.46	.86	.20
Both non-employed	.22	.00	.21	.00	.35
Household income	1.21	2.20	1.34	2.16	.81
Employment rate					
women	.52	.96	.59	.93	.37
men	.64	.96	.66	.93	.48
Human capital					
women	.77	1.00	.83	.92	.77
men	.89	.99	.90	.95	.87
Remote job share					
women	.00	.00	.48	.77	.00
men	.00	.00	.28	.50	.00

Notes.—Displayed are averages for households who migrate in the baseline economy and in the remote work scenario. The compositions are computed at the respective steady states.

Table 15: Steady state comparison: baseline economy vs. remote work scenario

	Calibrated remote		Fully remote	
	Women	Men	Women	Men
Earnings	1.35 %	.37 %	2.36 %	.79 %
Employment	.55 %	.07 %	1.08 %	.14 %
Local productivity	.26 %	.24 %	.54 %	.54 %
Human capital	.52 %	.08 %	.95 %	.13 %

Notes.—Differences are computed between the steady-state distribution of the remote work economy relative to the baseline economy. “Calibrated remote” refers to the remote economy as calibrated in Section 7.1, “fully remote” refers to the case where all jobs are remote.

productivity, reflected notably in male earnings.

Table 15 summarizes the steady-state impact on earnings, relative to the baseline. On average, earnings in the remote economy rise by 1.35% for women and 0.37% for men.

Comparison with losses from colocation friction We conclude by comparing the effect of remote work to that of eliminating the colocation friction. Both counterfactuals prevent employment losses among trailing spouses. However, there are a few subtle differences.

First, unlike the correlated matching counterfactual — which reallocates job offers across households without altering the aggregate matching frontier — remote work expands the feasible set of matches.²⁷ Second, remote work relaxes the colocation friction only for employed

²⁷To see this, note that migration with a remote job is isomorphic to creating a new match without additional search effort by the worker and without creating a new vacancy.

workers, whereas the correlated matching counterfactual also treats unemployed workers.²⁸ Third, and most importantly, because remote work is limited to specific occupations, its aggregate impact is reduced due to a smaller treatment scope.

To control for differences in treatment scope, we also simulate a “fully remote” economy, as reported in the final two columns of Table 15. Earnings gains in this scenario reach approximately 90% of those observed when eliminating the colocation friction (cf., Table 12). The remaining gap reflects the continued impact of the friction on unemployed workers, partially offset by the expanded matching frontier of remote work.

In conclusion, remote work has the potential to eliminate the colocation friction for households most exposed to it, largely replicating the gains from directly removing it. In practice, accounting for occupational constraints on remote feasibility, remote work can cut average earnings losses attributed to the colocation friction by up to 50%.

8 Concluding Remarks

This paper develops a spatial framework to study how search frictions shape job search, migration, and labor market outcomes of dual-earner households. We estimate the model for the U.S. labor market. The estimated model reproduces observed gender gaps in wages and employment without targeting them during the estimation.

We highlight the “colocation friction” as the key constraint distinguishing dual-earner households from single earners. The colocation friction amplifies gender inequality after migration, reduces migration rates — particularly among “power couples” —, and lowers steady-state earnings for both genders. We also examine how the rise of remote work mitigates the colocation friction, with the potential to halve these earnings losses in the long run.

Our framework is among the first to integrate dual-earner job search into a spatial labor market model. It is distinguished from the existing literature by its analytical tractability, which enables a large-scale estimation at the commuting-zone level. The estimated framework delivers rich predictions about dual-earner households’ careers and gender disparities in employment and earnings.

²⁸It is straightforward to show that the colocation friction is slack for all searches if at least one spouse has a remote job.

References

- Albrecht, James, Pieter A. Gautier & Susan Vroman** (2006). "Equilibrium Directed Search with Multiple Applications". *Review of Economic Studies* 73 (4), pp. 869–891.
- Alonzo, Davide, Nezih Guner & Claudio Luccioletti** (2023). "Segregation and Sorting of U.S. Households: Who Marries Whom and Where?"
- Autor, David H. & David Dorn** (2013). "The Growth of Low-Skill Service Jobs and the Polarization of the US Labor Market". *American Economic Review* 103 (5), pp. 1553–97.
- Bagga, Sadhika, Lukas Friedrich Mann, Aysegül Şahin & Giovanni L. Violante** (2025). "Job Amenity Shocks and Labor Reallocation". NBER Working Paper (33787).
- Baley, Isaac, Ana Figueiredo & Robert Ulbricht** (2022). "Mismatch Cycles". *Journal of Political Economy* 130 (11), pp. 2943–2984.
- Barrero, José María, Nicholas Bloom & Steven J. Davis** (2023). "The Evolution of Work from Home". *Journal of Economic Perspectives* 37 (4), pp. 23–50.
- Berresheim, Ursula** (2025). "Work from Home, Work for Less? How Workspace Flexibility Affects Mothers' Careers".
- Bloom, Nicholas, James Liang, John Roberts & Zhichun Jenny Ying** (2015). "Does Working from Home Work? Evidence from a Chinese Experiment". *The Quarterly Journal of Economics* 130 (1), pp. 165–218.
- Braun, Christine, Charlie Nusbaum & Peter Rupert** (2021). "Labor market dynamics and the migration behavior of married couples". *Review of Economic Dynamics* 42, pp. 239–263.
- Brinatti, Agostina, Alberto Cavallo, Javier Cravino & Andres Drenik** (2021). "The International Price of Remote Work". NBER Working Paper (29437).
- Cahuc, Pierre, Fabien Postel-Vinay & Jean-Marc Robin** (2006). "Wage Bargaining with On-the-Job Search: Theory and Evidence". *Econometrica* 74 (2), pp. 323–364.
- Chetty, Raj, John N. Friedman, Nathaniel Hendren, Maggie R. Jones & Sonya R. Porter** (2025). "The Opportunity Atlas: Mapping the Childhood Roots of Social Mobility". *American Economic Review*, forthcoming.
- Chetty, Raj, Michael Stepner, Sarah Abraham, Shelby Lin, Benjamin Scuderi, Nicholas Turner, Augustin Bergeron & David Cutler** (2016). "The Association Between Income and Life Expectancy in the United States, 2001–2014". *JAMA* 315 (16), pp. 1750–1766.
- Cortés, Patricia, Jessica Pan, Laura Pilossoph, Ernesto Reuben & Basit Zafar** (2023). "Gender Differences in Job Search and the Earnings Gap: Evidence from the Field and Lab". *The Quarterly Journal of Economics* 138 (4), pp. 2069–2126.
- Costa, Dora L. & Matthew E. Kahn** (2000). "Power Couples: Changes in the Locational Choice of the College Educated, 1940–1990". *The Quarterly Journal of Economics* 115 (4), pp. 1287–1315.
- DellaVigna, Stefano, Jörg Heining, Johannes F. Schmieder & Simon Trenkle** (2021). "Evidence on Job Search Models from a Survey of Unemployed Workers in Germany". *The Quarterly Journal of Economics* 137 (2), pp. 1181–1232.
- Dey, Matthew & Christopher Flinn** (2008). "Household search and health insurance coverage". *Journal of Econometrics* 145 (1), pp. 43–63.
- Din, Alexander & Ron Wilson** (2020). "Crosswalking ZIP Codes to Census Geographies: Geoprocessing the U.S. Department of Housing and Urban Development's ZIP Code Crosswalk Files". *Cityscape: A Journal of Policy Development and Research* 22 (1).
- Dingel, Jonathan I. & Brent Neiman** (2020). "How many jobs can be done at home?" *Journal of Public Economics* 189, p. 104235.
- Doepke, Matthias & Michèle Tertilt** (2016). "Families in Macroeconomics". In: ed. by John B. Taylor & Harald Uhlig. Vol. 2. *Handbook of Macroeconomics*. Elsevier, pp. 1789–1891.
- Emanuel, Natalia & Emma Harrington** (2024). "Working Remotely? Selection, Treatment, and the Market for Remote Work". *American Economic Journal: Applied Economics* 16 (4), pp. 528–59.
- Findeisen, Sebastian, Sang Yoon (Tim) Lee, Tommaso Porzio & Wolfgang Dauth** (2021). "Transforming Institutions: Labor Reallocation and Wage Growth in a Reunified Germany". *Working Paper*.
- Flabbi, Luca & James Mabli** (2018). "Household Search or Individual Search: Does It Matter?" *Journal of Labor Economics* 36 (1), pp. 1–46.

- Galenianos, Manolis & Philipp Kircher** (2009). "Directed Search with Multiple Job Applications". *Journal of Economic Theory* 144 (2), pp. 445–471.
- Galenianos, Manolis, Philipp Kircher & Gábor Virág** (2011). "Market Power and Efficiency in a Search Model". *International Economic Review* 52 (1), pp. 85–103.
- Gemici, Ahu** (2023). "Family Migration and Labor Market Outcomes".
- Gibbs, Michael, Friederike Mengel & Christoph Siemroth** (2023). "Work from Home and Productivity: Evidence from Personnel and Analytics Data on Information Technology Professionals". *Journal of Political Economy Microeconomics* 1 (1), pp. 7–41.
- Glaeser, Nina, Joan Monras & Milan Quentel** (2025). "Spousal Sorting, Spatial Misallocation, and the Gender Wage Gap".
- Guler, Bulent, Fatih Guvenen & Giovanni L. Violante** (2012). "Joint-Search Theory: New Opportunities and New Frictions". *Journal of Monetary Economics* 59 (4), pp. 352–369.
- Guner, Nezih, Remzi Kaygusuz & Gustavo Ventura** (2020). "Child-Related Transfers, Household Labour Supply, and Welfare". *The Review of Economic Studies* 87 (5), pp. 2290–2321.
- Herkenhoff, Kyle, Gordon Phillips & Ethan Cohen-Cole** (2023). "How Credit Constraints Impact Job Finding Rates, Sorting, and Aggregate Output". *The Review of Economic Studies* 91 (5), pp. 2832–2877.
- Hosios, Arthur J.** (1990). "On the Efficiency of Matching and Related Models of Search and Unemployment". *The Review of Economic Studies* 57 (2), p. 279.
- Huckfeldt, Christopher** (2022). "Understanding the Scarring Effect of Recessions". *American Economic Review* 112 (4), pp. 1273–1310.
- Jarosch, Gregor** (2023). "Searching for Job Security and the Consequences of Job Loss". *Econometrica* 91 (3), pp. 903–942.
- Jayachandran, Seema, Lea Nassal, Matthew J. Notowidigdo, Marie Paul, Heather Sarsons & Elin Sundberg** (2024). "Moving to Opportunity, Together". NBER Working Paper (32970).
- Jovanovic, Boyan** (1979). "Job Matching and the Theory of Turnover". *Journal of Political Economy* 87 (5), pp. 972–990.
- (1984). "Matching, Turnover, and Unemployment". *Journal of Political Economy* 92 (1), pp. 108–122.
- Jung, Philip & Moritz Kuhn** (2019). "Earnings Losses and Labor Mobility over the Life Cycle". *Journal of the European Economic Association* 17 (3), pp. 678–724.
- Kaplan, Greg & Sam Schulhofer-Wohl** (2017). "Understanding the Long-Run Decline in Interstate Migration". *International Economic Review* 58 (1), pp. 57–94.
- Kennan, John & James R. Walker** (2011). "The Effect of Expected Income on Individual Migration Decisions". *Econometrica* 79 (1), pp. 211–251.
- Kircher, Philipp** (2009). "Efficiency of Simultaneous Search". *Journal of Political Economy* 117 (5), pp. 861–913.
- Lange, Fabian & Theodore Papageorgiou** (2020). "Beyond Cobb-Douglas: Flexibly Estimating Matching Functions with Unobserved Matching Efficiency". NBER Working Paper (26972).
- Lessem, Rebecca** (2017). "Mexico–U.S. Immigration: Effects of Wages and Border Enforcement". *The Review of Economic Studies* 85 (4), pp. 2353–2388.
- Lise, Jeremy & Jean-Marc Robin** (2017). "The Macrodynamics of Sorting between Workers and Firms". *American Economic Review* 107 (4), pp. 1104–1135.
- Lundberg, Shelly & Robert A. Pollak** (2003). "Efficiency in Marriage". *Review of Economics of the Household* 1 (3), pp. 153–167.
- Maurer, Roy** (2017). *Americans Most Often Move for Work*. SHRM. URL: <https://www.shrm.org/topics-tools/news/talent-acquisition/americans-often-move-work> (visited on 11/21/2025).
- Menzio, Guido & Shouyong Shi** (2010). "Block Recursive Equilibria for Stochastic Models of Search on the Job". *Journal of Economic Theory* 145 (4), pp. 1453–1494.
- (2011). "Efficient Search on the Job and the Business Cycle". *Journal of Political Economy* 119 (3), pp. 468–510.
- Menzio, Guido, Irina A. Telyukova & Ludo Visschers** (2016). "Directed Search over the Life Cycle". *Review of Economic Dynamics* 19, pp. 38–62.
- Mincer, Jacob** (1978). "Family Migration Decisions". *Journal of Political Economy* 86 (5), pp. 749–773.
- Pilossoph, Laura & Shu Lin Wee** (2021). "Household Search and the Marital Wage Premium". *American Economic Journal: Macroeconomics* 13 (4), pp. 55–109.

- Piyapromdee, Suphanit** (2020). “The Impact of Immigration on Wages, Internal Migration, and Welfare”. *The Review of Economic Studies* 88 (1), pp. 406–453.
- Rabinovich, Stanislav & Ronald Wolthoff** (2022). “Misallocation inefficiency in partially directed search”. *Journal of Economic Theory* 206, p. 105559.
- Román, Olatz** (2025). “The Geography of Jobs and Couple Migration”.
- Rueda, Valeria & Guillaume Wilemme** (2025). “Career Paths with a Two-Body Problem: Colocation and Gendered Professional Crossroads”.
- Sahin, Ayşegül, Joseph Song, Giorgio Topa & Giovanni L. Violante** (2014). “Mismatch Unemployment”. *American Economic Review* 104 (11), pp. 3529–3564.
- Schaal, Edouard** (2017). “Uncertainty and Unemployment”. *Econometrica* 85 (6), pp. 1675–1721.
- Shimer, Robert** (2005). “The Cyclical Behavior of Equilibrium Unemployment and Vacancies”. *American Economic Review* 95 (1), pp. 25–49.
- Snyder, J. P.** (1982). *Map Projections Used by the U.S. Geological Survey*. Geological Survey United States: Geological Survey bulletin. U.S. Government Printing Office.
- Venator, Joanna** (2025). “Dual-Earner Migration Decisions, Earnings, and Unemployment Insurance”.
- Wright, Randall, Philipp Kircher, Benoît Julien & Veronica Guerrieri** (2021). “Directed Search: A Guided Tour”. *Journal of Economic Literature* 59 (1), pp. 90–148.

A Mathematical Appendix

A.1 Proof of Proposition 1

Let $f_{i,q} = \kappa_{i,q} \lambda(\theta_{\psi_{i,q}})$. For a given value function, search policies in the correlated matching benchmark solve

$$\max_{\{f_{i,q}, \omega_q, y_{i,q}\}} \left\{ \sum_{i,q} (f_{i,q} - \omega_q) \Delta V_{i,q}(\mathbf{e}, \mathbf{s}, r) + \sum_q \omega_q \Delta V_q^{\text{corr}}(\mathbf{e}, \mathbf{s}, r) - \sum_{i,q} f_{i,q} y_{i,q} \right\}$$

subject to (2), (3), (7) and (8). Observe that the objective is separable across q and is linear in $\{\omega_q\}$. Thus, for any q , ω_q is optimally set to one of the boundaries in (8), with the upper boundary being strictly optimal if and only if

$$\Delta V_q^{\text{corr}}(\mathbf{e}, \mathbf{s}, r) > \sum_i \Delta V_{i,q}(\mathbf{e}, \mathbf{s}, r).$$

This proves Proposition 1.

A.2 Kolmogorov Forward Equation

Collect all job-finding rates $\{f_{i,q}(\mathbf{e}, \mathbf{s}, r)\}$ along with all endogenous separations into μ , let n denote the replacement process of retiring households by new ones, and define $\sigma \equiv \mu + \pi + n$. Then the cross-sectional distribution, $g_t(\mathbf{e}, \mathbf{s}, r)$, evolves according to the following differential equation:

$$\frac{dg_t}{dt}(\mathbf{e}', \mathbf{s}', r') = \sum_{\mathbf{e}, \mathbf{s}, r} \sigma(\mathbf{e}', \mathbf{s}', r' | \mathbf{e}, \mathbf{s}, r) g_t(\mathbf{e}, \mathbf{s}, r). \quad (\text{A.1})$$

From (A.1), we may obtain the steady state distribution by setting $dg = 0$ subject to $\sum g = 1$.

In practice, when estimating the model, we embed the steady-state condition as a constraint into our moments-matching algorithm when computing the distribution of location preference shocks with the smallest total prevalence subject to matching the cross-sectional distribution of households over commuting zones.

B Data Appendix

B.1 Data Sources

This appendix describes the data sources that we use in calibrating our model.

American Community Survey (ACS) We construct our ACS sample using the years 2010–2019, restricting attention to individuals aged 18–64, who live in the 48 contiguous states (i.e., excluding Alaska, Hawaii, and Puerto Rico), who are part of a couple (married or cohabiting), and whose partner was also surveyed. 1990 Census Occupation codes are mapped into the occupation classification by Autor & Dorn (2013) using their crosswalk. We deflate wages to 2010 USD using the CPI. To obtain median wages and occupation-shares by commuting zone (CZ), we adopt crosswalks by Autor & Dorn (2013) to aggregate data from Public Use Micro Areas (PUMAs) to the CZ level.

Current Population Survey (CPS) We construct our CPS sample replicating the sample restrictions used for the ACS. 1990 Census Occupation codes are mapped into the occupation classification by Autor & Dorn (2013) using their crosswalk.

Panel Study of Income Dynamics (PSID) We construct our PSID sample to replicate the ACS sample restrictions as closely as possible. We include all existing PSID waves between 2010 and 2019 (2011, 2013, 2017, and 2019). All other sample restrictions used for the ACS are applied identically.

Opportunity Atlas We use CZ-level data from the Opportunity Atlas (Chetty et al. 2025). The Opportunity Atlas draws on various U.S. data sources and aggregates them at the CZ level. For a detailed description of several variables that we draw from the Opportunity Atlas see also Chetty et al. (2016).

Web-scraped data We use web scraping to obtain CZ-level information on local weather and climate conditions, crime rates, walkability scores, measures of beach access and quality, school and hospital quality, and local government expenditures. Specifically, we scrape information published on bestplaces.net, usnews.com, walkscore.com, and watersgeo.epa.gov. The raw data are aggregated at the county and ZIP code levels, respectively. To aggregate these data to CZs, we use crosswalks by Autor & Dorn (2013) and Din & Wilson (2020). For a description of all web-scraped variables and their sources see Table A.I in Appendix B.3.

Geolocation data To locate CZs in space, we use county centroid geographic coordinate system (GCS) coordinates provided by simplemaps.com. We apply the Albers equal-area projection to transform GCS coordinates into Albers equal-area (AEA) coordinates.^{A1} The advantage of using AEA coordinates is that they are Cartesian; i.e., geographic distances can be expressed as Euclidean “straight-line” distances, which allows us to adopt the crosswalk by Autor & Dorn (2013) to aggregate county coordinates to population weighted CZ centroids and further aggregate commuting zones as described in Appendix B.4.

B.2 Measuring Labor Market and Migration Flows

Labor Market Flows We measure labor market flows by using the rotating panel structure of the CPS. The CPS is a monthly survey conducted among a nationally representative sample of households. Leveraging matched individual records for consecutive months, we compute monthly transition frequencies between employment states, conditioning on sex and household occupations.

Migration Flows We measure migration flows using ACS data on where individuals reside when surveyed and their residence one year prior. In particular, the ACS records the Public Use Micro Area (PUMA) individuals reside in when surveyed and the Migration Public Use Micro Area (MIGPUMA) one year prior. MIGPUMAs are constructed from one or multiple PUMAs. We map MIGPUMAs into PUMAs using a crosswalk published by usa.ipums.org, and map PUMAs into CZs using crosswalks developed by Autor & Dorn (2013). In computing across-CZ migration rates, we adopt a conservative approach, counting as cross-CZ migration only a change in residence from a MIGPUMA to a PUMA that have zero overlap in the CZs they intersect with. To obtain spatial distances between migration origin and destination, we use spatial coordinates of population weighted CZ centroids. For differences in population size we use population counts as recorded in the ACS. We aggregate to the PUMA and MIGPUMA level, respectively, using the crosswalks mentioned above together with a crosswalk from counties to CZs also by Autor & Dorn (2013).

B.3 Measuring Amenities

This appendix describes the data inputs and results of regression 11, which we use to convert our CZ-level amenity data into income-equivalent units. Table A.I describes the definition and data source of each amenity in our data. Table A.II summarizes the estimation results of regression (11). Most coefficient estimates are statistically significant at the 1% level. The adjusted R^2 of the regression is 86%.

B.4 Merging Commuting Zones

This appendix describes the algorithm by which we merge CZs that are close geographically and in terms of observed characteristics. Geographic distances between CZs are computed based on AEA coordinates of CZ centroids. We define closeness in terms of all observed CZ characteristics that feed into our calibration; i.e., rents, amenities with and without children (converted to income equivalent units as described in Section 4.2),

^{A1}We follow Snyder (1982) in using the AEA standard parallels 29.5° and 45.5° north.

Table A.I: Description of amenities data

Variable	Description	Data Source
Population density	Number of people per square mile.	Atlas
Local government expenditures	Total local government expenditures per capita, USD per annum.	Atlas
Crime rate	Annual crime rate per million people.	Atlas
Hospital quality	State's ranking in health care quality. State data is applied to each CZ in the state. Scale: 1–10, 10 being highest quality.	usnews.com
Walkability score	Score based on availability of infrastructure and number of restaurants, bars and coffee shops within 5 minutes walking distance. More choices within a radius yields a higher score. Scale: 0–100, 100 being the highest walkability. Aggregated to CZ level from Zip Code Level.	walkscore.com
No. of top tier beaches	Beaches in the most popular tier, sampled one month before swim season.	watersgeo.epa.gov
Annual precipitation (inches)	Annual inches of precipitation. Aggregated to CZ level from county level.	betsplaces.net
Annual snowfall (inches)	Annual inches of snowfall. Aggregated to CZ level from county level.	betsplaces.net
Average July high temperature (°F)	Aggregated to CZ level from county level.	betsplaces.net
Average school score	Index that combines student proficiency on state standardized tests, SAT/ACT performance, and high school graduation rates. Scale: 1–10, 10 being the best possible score.	greatschools.org
Hightschool dropout rate (income adjusted)	Residual from a regression of high school dropout rates on household income per capita in 2000.	Atlas
School expenditure per student	Average expenditures per student in public schools, USD per annum.	Atlas

Notes.—We winsorize annual snowfall and local government expenditures at the 99th percentile to reduce the impact of outliers. Missing observations are filled in as follows: For two CZs in New Jersey, school expenditures are filled in with state-level data from nces.ed.gov. For 16 CZs in Florida, and 18 CZs in Illinois, crime rates are filled in with state-level data from ucr.fbi.gov. For one CZ in Connecticut and three CZs in Vermont, high school dropout rates are imputed using linear predictions from a regression of dropout rates on all other amenity variables.

Table A.II: Empirical relationship between amenities and rent

Dependent variable: Annual rent in \$	Coefficient estimate	Standard error	P-value
Median household wage (passthrough rate, ϵ)	.161	.008	.000
Population density (people/mile ²)	.501	.082	.000
Local government expenditures (\$ per capita)	1.419	.107	.000
Crime rate (per mio. people)	-42.558	23.728	.073
Hospital quality	27.475	2.336	.000
Walkability score	47.912	4.518	.000
No. of top tier beaches	54.192	15.877	.001
Annual precipitation (inches)	-15.408	5.465	.005
Annual snowfall (inches)	-42.696	3.262	.000
Avg. July high temperature (°F)	112.652	20.411	.000
Avg. July high temperature squared	-.065	.012	.000
Share of HHs with children, \bar{k}_r (%)	-16.898	28.544	.554
$\bar{k}_r \times$ Avg. school score	4.552	2.591	.079
$\bar{k}_r \times$ Highschool dropout rate (income adjusted)	-1.668	.850	.050
$\bar{k}_r \times$ School expenditure per student (\$ per annum)	-.001	.001	.405

Notes.—Displayed are coefficient estimates of the relationship between amenities and rents on the CZ level (equation (11)). Hospital quality is recorded on a 1–10 scale, 10 denoting the best possible score. The Walkability score is recorded on a 0–100 scale, 100 denoting highest walkability. The school score is recorded on a 1–10 scale, 10 denoting the best possible score. The regression includes 720 commuting zones (out of a total of 741) for which all amenities and annual rents are observed in our data. The adjusted R^2 of the regression is 0.86.

the local population counts of occupation vector \mathbf{o} , and gender \times occupation-specific median wages. As a joint measure of geographically proximity and similarity in observables of CZs, we use the weighted Euclidean norm

$$d_{CZ}(r, r') = \sqrt{\frac{1}{J} \sum_j \left(\frac{x_j(r) - x_j(r')}{\omega_j} \right)^2},$$

where $x_1(r)$ and $x_2(r)$ are AEA latitude and longitude and $\{x_j(r)\}_{j=3}^J$ are the remainder characteristics of CZ r . The weights $\{\omega_j\}$ correspond to the standard deviations of the observed characteristics across CZs, and across all pairwise combinations of CZs for the AEA coordinates.

Equipped with d_{CZ} and some cutoff \bar{d} , our algorithm proceeds as follows:

1. Start from the full list of CZs. Sort it in ascending order in terms of population size. Denote the resulting sorted list by $I = (r_0, r_1, \dots, r_K)$. Start from $k = 0$.
2. Find $l^* = \operatorname{argmin}_{l>k} d_{CZ}(r_k, r_l)$.
3. If $d_{CZ}(r_k, r_{l^*}) \leq \bar{d}$:
 - (a) Merge r_{l^*} with r_k (removing r_{l^*} from I). Update the characteristics of the newly merged CZ, $\{x_j(r_k)\}_{j=1}^J$, by summing population sizes and type- \mathbf{o} household population counts of r_k and r_{l^*} , and taking population-weighted averages of all other characteristics.

- (b) Iterate through $\{r_m : r_m \in I, m < k\}$ and merge each element r_m satisfying $d_{CZ}(r_m, r_k) \leq \bar{d}$ with r_k , following the steps outlined above to update the characteristics, $\{x_j(r_k)\}_{j=1}^J$, and removing r_m from I .
4. Increase k by 1 and proceed to the next element in I . Repeat steps 2–4 until $k = K$. The resulting I contains the list of merged CZs.

We set the cutoff to $\bar{d} = \frac{1}{3}$, implying that if two commuting zones are identical in all but one characteristic, then the most they can differ in that one characteristic is $\frac{1}{3}$ standard deviation. Starting from 720 CZs with non-missing data, our algorithm delivers a set of 546 merged CZs. The average geographic distance between the centroids of CZs merged by our algorithm is 108 kilometers. The average distance in terms of d_{CZ} is 0.21.

B.5 Additional Figures

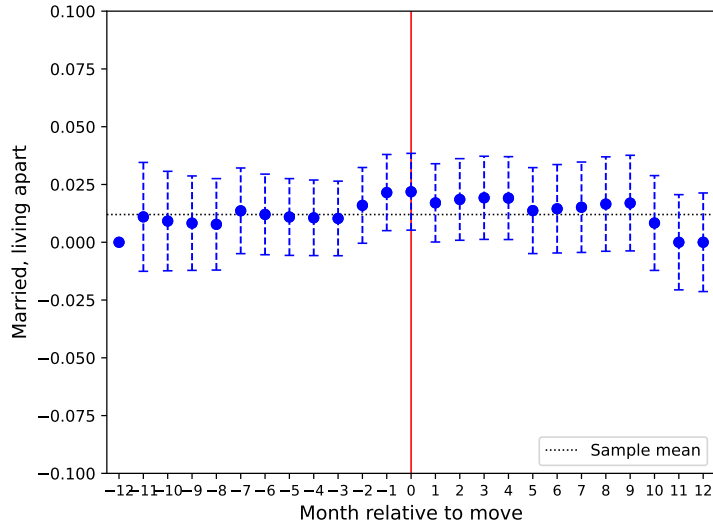


Figure A.I: The plot shows the share of couples who are married but living apart by month relative to migration, conditional on living together $t=-12$ months prior to migration. The sample is restricted to couples who were living together 12 months prior to migration. The dashed vertical lines indicate 95% confidence intervals. The dotted horizontal line shows the unconditional sample mean. Computed based on married couples in our PSID sample.